HELSINKI UNIVERSITY OF TECHNOLOGY

Department of Civil and Environmental Engineering

MIRVA KOSKINEN

ANISOTROPY AND DE-STRUCTURATION OF SOFT CLAYS

Master's Thesis submitted on 21/05/2001

SUPERVISOR: Docent MINNA KARSTUNEN

INSTRUCTOR: Lic.Sc. (Tech.) MATTI LOJANDER

HELSINKI UNIVERSITY OF TECHNOLOGY
DEPARTMENT OF CIVIL AND ENVIRONMENTAL ENGINEERING

ABSTRACT OF THE MASTER'S THESIS

Author:	Mirva Koskinen		
Thesis:	Anisotropy and de-structuration of soft clays		
Date:	21/05/2001	**Number of pages:**	81
Chair:	Soil Mechanics and Foundation Engineering	**Code:**	Rak-50
Supervisor:	Docent Minna Karstunen		
Instructor:	Lic.Sc. (Tech.) Matti Lojander		

This thesis was done in the Laboratory of Soil Mechanics and Foundation Engineering at the Helsinki University of Technology (HUT) and at the University of Glasgow (GU). This work is a part of a project called "Modelling of the mechanical behaviour of naturally anisotropic soft soils" funded by the Finnish Academy. The secondment in Glasgow was enabled by the project "Soft Clay Modelling for Engineering Practice", which is a research training network funded by the European Commission.

The aim of this thesis was to examine two constitutive soil models for soft, normally or lightly overconsolidated clays. The first model S-CLAY1, developed jointly by GU and HUT, takes into account the natural anisotropy and the changes in it due to subsequent loading. The second model SS-CLAY1, proposed by Wheeler and his co-workers at GU, combines the anisotropy with the effects of structure in the soil and models the degradation of bonding due to loading, a phenomenon called de-structuration. The aim of the latter model is to describe the behaviour of soil realistically and even though a component that takes the structure into account has been included, the amount of parameters is still reasonable. In the future, the model SS-CLAY1 is hoped to be a useful tool for practical design purposes.

In this work both models were studied with the help of laboratory tests. The test program included triaxial tests on reconstituted samples in addition to tests on natural samples. One objective was to develop a procedure for making consistent reconstituted samples. The determination of some parameters alternatively from oedometer tests was also studied. The triaxial tests were simulated with Microsoft Excel by using routines developed by the author based on incremental elasto-plastic approach in order to compare the model predictions with the observations.

It was noticed that the anisotropic model, S-CLAY1, is suitable for simulating nearly isotropic tests on natural clays, because no significant de-structuration takes place in such cases. The combined model, SS-CLAY1, was found to be promising for simulating tests with various anisotropic stress paths. However, it was not possible to find one single parameter combination that would produce good predictions for all simulated tests. The results also indicate that the assumption of an associated flow rule should perhaps be questioned. Further model development is hence needed.

TEKNILLINEN KORKEAKOULU
RAKENNUS- JA YMPÄRISTÖTEKNIIKAN OSASTO

DIPLOMITYÖN TIIVISTELMÄ

Tekijä: Mirva Koskinen

Diplomityö: Anisotropy and de-structuration of soft clays

Päivämäärä: 21.5.2001 **Sivumäärä:** 81
Professuuri: Pohjarakennus ja maamekaniikka **Koodi:** Rak-50

Valvoja: Dosentti Minna Karstunen
Ohjaaja: TkL Matti Lojander

Tämä työ on tehty Teknillisen korkeakoulun Pohjarakennuksen ja maamekaniikan laboratoriossa sekä Glasgown yliopistossa. Työ on osa Suomen Akatemian rahoittamaa projektia "Modelling of the mechanical behaviour of naturally anisotropic soft soils". Työskentely Glasgowssa tapahtui projektin "Soft Clay Modelling for Engineering Practice" puitteissa, ja sen on rahoittanut Euroopan komissio.

Tässä työssä tarkasteltiin kahta uutta pehmeille, normaalisti tai lievästi ylikonsolidoituneille saville soveltuvaa konstitutiivista maamallia. Ensimmäinen malli S-CLAY1, joka on kehitetty Teknillisen korkeakoulun ja Glasgown yliopiston yhteistyönä, ottaa huomioon maan luonnollisen anisotropian ja kuormituksen siihen aiheuttamat muutokset. Toinen malli SS-CLAY1, jonka on kehittänyt Wheeler työtovereineen Glasgown yliopistossa, huomioi tämän lisäksi maan luonnossa syntyneen rakenteen ja kuormituksen aiheuttaman rakenteen vähittäisen tuhoutumisen eli destrukturaation. Jälkimmäisen mallin on tarkoitus kuvata maan käyttäytymistä realistisesti, ja vaikka siihen on lisätty rakenteen vaikutuksen huomioiva komponentti, ei parametrien määrä ole silti kasvanut kohtuuttomaksi. Jälkimmäisen mallin toivotaan tulevaisuudessa olevan käyttökelpoinen työkalu käytännön suunnittelutehtävissä.

Työssä tutkittiin molempia maamalleja laboratoriokokein. Koeohjelmaan kuului luonnontilaisten kolmiaksiaalikokeiden lisäksi myös kattava määrä sekoitetuille näytteille tehtyjä kolmiaksiaalikokeita. Yhtenä tarkoituksena oli myös kehittää sekoitettujen näytteiden valmistukseen soveltuva tekniikka. Lisäksi tutkittiin joidenkin parametrien vaihtoehtoista määritystä ödometrikokein. Maamallien toimintaa tutkittiin simuloimalla tehtyjä kolmiaksiaalikokeita Microsoft Excel taulukkolaskentaohjelmalla. Muodonmuutokset laskettiin pienten kuormituslisäysten avulla tekijän kokoamassa laskentataulukossa.

Anisotrooppinen malli S-CLAY1 todettiin soveltuvaksi lähes isotrooppisten kokeiden simulointiin, koska niissä ei tapahdu merkittävää rakenteen rikkoutumista. Anisotropian ja rakenteen vaikutuksen yhdistävä malli SS-CLAY1 todettiin lupaavaksi ja huomattiin sen soveltuvan parhaiten anisotrooppisesti kuormitettujen kokeiden simulointiin. Yhtä parametriyhdistelmää, jolla voitaisiin ennustaa hyvin kaikkia kokeita, ei kuitenkaan löydetty. Tulosten mukaan mallin heikko kohta on oletus assosiatiivisesta myötösäännöstä. Tulokset voisivat parantua epäassosiatiivisen myötösäännön avulla. Mallin jatkokehittelyä tarvitaankin edelleen.

PREFACE

I would like to thank Dr Minna Karstunen and Lic.Sc. (Tech.) Matti Lojander for the guidance and support that they have given me for this Master's thesis. I would also like to thank Professor Simon Wheeler from University of Glasgow for his time and advice that has been very valuable for me during this project. Also the help of Kevin McGinty in the laboratory at University of Glasgow was essential.

In addition, I would like to thank the personnel of the Laboratory of Soil Mechanics and Foundation Engineering at the Helsinki University of Technology as well as the staff of the Department of Civil Engineering at the University of Glasgow and everybody else who have supported me in my work.

Espoo, the 21st of May 2001

Mirva Koskinen

LIST OF SYMBOLS

A	Area of the sample, cm^2
a	Model parameter of SS-CLAY1, describes the rate the bonds are breaking at within the soil
b	Model parameter of SS-CLAY1, describes the relative effectiveness of the plastic strains in breaking the bonds within the soil
Cl-%	Clay content
d	Diameter of the sample, cm
e	Void ratio
f	Yield function, kPa^2
G'	Elastic shear modulus, kPa
G_s	Specific density
g	Plastic potential function, kPa^2
H	Hardening modulus
H_f	Height of the reconstituted sample after one-dimensional consolidation, cm
H_i	Height of the reconstituted sample before one-dimensional consolidation, cm
H_s	Height of soil particles, cm
Hm-%	Organic content
h	Height of the sample, cm
I_p	Plasticity index

K_0	Coefficient of the earth pressure at rest
k	Permeability coefficient, m/s
n	Porosity, %
OCR	Overconsolidation ratio
p	Mean stress, kPa
p'	Mean effective stress, kPa
p'_m	Size of the yield curve, kPa
p'_{mi}	Size of the intrinsic yield curve, kPa
q	Deviator stress, kPa
S_r	Degree of saturation, %
S_t	Sensitivity
s_k	Shear strength, kN/m^2
u_w	Pore water pressure, kPa
V	Volume of the sample, cm^3
v	Specific volume
w	Water content, %
w_L	Liquid limit, %
w_p	Plastic limit, %
x	Parameter that controls the extent of the bonding effect within soil
z	Depth, m

α	Scalar value of the fabric tensor, defines the orientation of the yield curve
β	Model parameter in S-CLAY1 and SS-CLAY1, describes the relative effectiveness of plastic strains in rotating the yield curve towards its target inclination
ε_d	Shear strain, %
ε_d^e	Elastic component of shear strain, %
ε_d^p	Plastic component of shear strain, %
ε_v	Volumetric strain, %
ε_v^e	Elastic component of volumetric strain, %
ε_v^p	Plastic component of volumetric strain, %
ε_1, ε_3	Principal strains, %
φ'	Effective friction angle, ^{o}
Γ	Specific volume of soil at critical state when p'=1.0 kPa
γ	Unit weight, kN/m^3
η	Stress ratio
κ	Slope of the swelling line in ln p': v plane
Λ	Plastic multiplier
λ	Slope of the normal compression line in ln p': v plane
M	Parameter of critical state, slope of the critical state line
μ	Model parameter in S-CLAY1 and SS-CLAY1, describes the rate at which α rotates towards its target value

ν	Poisson ratio
ρ_s	Particle density, g/cm^3
σ_p	Preconsolidation pressure, kPa
σ'_1, σ'_3	Principal effective stresses, kPa

TABLE OF CONTENTS

1. INTRODUCTION

In geotechnical practice, the design methods used are usually rather conservative and inaccurate even if there have been some improvements in that area. This, together with the fact that many urban areas are more and more densely populated these days, and therefore areas with difficult geology have been adopted for construction, require design tools that are more efficient both in terms of economy and safety.

This work was done as a part of a project called "Modelling the mechanical behaviour of naturally anisotropic soft soils", which is funded by the Finnish Academy. It is also a part of collaboration between the Helsinki University of Technology and the University of Glasgow within a research training network called "Soft Clay Modelling for Engineering Practice", which is funded by the European Commission.

The purpose of both projects is to develop better design tools for practical geotechnical design. As part of the project funded by the Finnish Academy, a new anisotropic elasto-plastic soil model S-CLAY1 for soft, normally or lightly overconsolidated soils was developed by Wheeler and his co-workers at Helsinki University of Technology and University of Glasgow. Comparison of the model predictions with the experimental data indicated that this model still needed some adjustments as for taking the effect of the soil structure into account. Therefore, a new model called SS-CLAY1 that combines the de-structuration effect with the anisotropic model S-CLAY1 was proposed by Wheeler (2000). Both models are described in Chapter 2.

Aim of this work was to analyse the soil behaviour with a constitutive model that takes both anisotropy and the effect of soil structure into account. The constitutive model is applied particularly to experimental results of POKO clay.

The first objective of this work was to study the preparation process of reconstituted samples of soft clay, and to test the samples in laboratory in triaxial apparatus. Material used for the purpose is POKO clay from near the town of Porvoo in Finland, but in addition, Bothkennar clay from Scotland was used for studying the sample preparation technique and the use of reconstituted samples in triaxial testing. The tests were carried out at University of Glasgow on Bothkennar clay and at Helsinki University of Technology on POKO clay. The sample preparation procedure is explained in detail in

Chapter 4. The test results of Bothkennar clay are presented in Section 4.1.3 and the results of POKO clay in Section 5.3.

The second objective of this work was to test natural, undisturbed soil samples in order to have test data of natural soils for comparison. POKO clay was again used as the material and these test results are presented in Section 5.1.

The third objective was to simulate the tests on reconstituted and natural samples of POKO clay with two models, with anisotropic model S-CLAY1 and with the model where de-structuration effect is combined with the anisotropy, SS-CLAY1. These simulations were done with Microsoft Excel by using routines developed by the author based on incremental elasto-plastic approach. Simulations for all tests can be found in Chapter 5 and conclusions and recommendations for further work are presented in Chapter 6.

2. ANISOTROPIC MODEL (S-CLAY1)

2.1 Background

The microstructure of clay is anisotropic by nature due to the asymmetric shape of the clay platelets, sedimentation and consolidation process, but most of the early models that have been developed assume soil as isotropic. This leads to unrealistic predictions of the behaviour of soil. One of the most commonly used isotropic elasto-plastic constitutive models is Modified Cam Clay (Roscoe and Burland 1968).

In recent years many anisotropic elasto-plastic soil models have been proposed (Banerjee and Yousif 1986, Dafalias 1987, Davies and Newson 1993, Whittle and Kavvadas 1994, Pestana and Whittle 1999). However, some of these models, like the two latter ones, are very complex and the model parameter determination may require non-standard laboratory tests. Other models predict unrealistic behaviour for some stress paths. This leads to problems in practical applications.

This chapter describes the anisotropic elasto-plastic model S-CLAY1 proposed by Wheeler and his co-workers for modelling soft, normally or lightly overconsolidated clay. This model is an extension to critical state models, and it describes anisotropy of plastic behaviour with a rotational component of hardening.

2.2 Model formulation

In triaxial space the stress state is described with deviator stress q and mean effective stress p', defined as:

$$q = \sigma'_1 - \sigma'_3 \tag{2.1}$$

$$p' = \frac{1}{3}\left(\sigma'_1 + 2\sigma'_3\right) \tag{2.2}$$

where σ'_1 and σ'_3 are the principal effective stresses.

Inside the yield surface behaviour of soil is assumed elastic, but when the stress state in p':q plane goes beyond the yield surface, plastic deformations begin to take place and

the yield surface starts to expand. Because plastic deformations are assumed to be dominating, elastic behaviour of soil is, for simplicity, thought to be isotropic and is described by the same elastic relationship as in Modified Cam Clay:

$$\begin{bmatrix} d\varepsilon_v^e \\ d\varepsilon_d^e \end{bmatrix} = \begin{bmatrix} \frac{\kappa}{vp'} & 0 \\ 0 & \frac{1}{3G'} \end{bmatrix} \begin{bmatrix} dp' \\ dq \end{bmatrix} \tag{2.3}$$

where $d\varepsilon_v^e$ is the increment of elastic volumetric strain, $d\varepsilon_d^e$ is the increment of elastic deviatoric strain, v is specific volume, κ is the slope of the swelling line in ln p':v plane and G' is the effective shear modulus.

In S-CLAY1, yield function is a sheared ellipse, which was originally proposed independently by Dafalias (1987) and Korhonen and Lojander (1987), and is defined in triaxial space by

$$f = (q - \alpha p')^2 - (M^2 - \alpha^2)(p'_m - p')p' = 0 \tag{2.4}$$

where M is the value of the stress ratio η=q/p' in critical state, p'_m defines the size of the yield curve and α defines the inclination of the yield curve. The yield curve is presented in Figure 2.1. The yield curve has hence horizontal gradients at the intersection with the critical state line both in triaxial compression and extension, and a vertical gradient at the intersection with the α line.

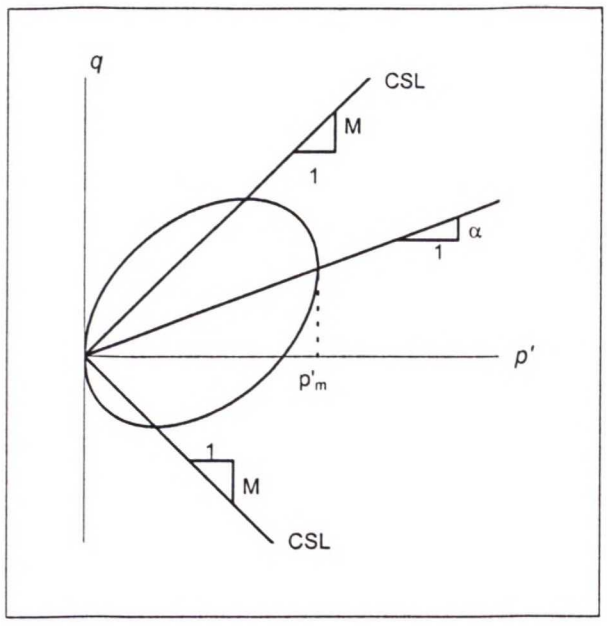

Figure 2.1. *Initial yield curve.*

There are two hardening laws in S-CLAY1, the first of which describes changes in size of the yield curve. It is analogous to the hardening law of Modified Cam Clay.

$$dp'_m = \frac{vp'_m}{\lambda - \kappa} d\varepsilon^p_v \tag{2.5}$$

where λ is the slope of the normal compression line.

The second hardening law is rotational hardening law, which describes changes in the inclination of the yield curve. The rotational hardening law was originally proposed by Wheeler (1997), and it can be expressed in generic form:

$$d\alpha = \mu[(\chi_v(\eta) - \alpha) < d\varepsilon^p_v > + \beta(\chi_d(\eta) - \alpha) \mid d\varepsilon^p_d \mid] \tag{2.6}$$

where $\chi_v(\eta)$ and $\chi_d(\eta)$ are the target values of α for plastic volumetric strains and plastic shear strains, respectively, which depend on the value of η. Näätänen et al. (1999) proposed based on tests on Otaniemi clay that

$$\chi_v(\eta) = \frac{3\eta}{4} \tag{2.7}$$

$$\chi_d(\eta) = \frac{\eta}{3} \tag{2.8}$$

Tests on some other clays suggest that this can be assumed more generally as well. Constants μ and β are soil parameters that describe the rate of α heading towards the target value and the relative effectiveness of plastic deviatoric strains and plastic volumetric strains in rotating the yield curve, respectively.

The Macaulay brackets on the plastic volumetric strain increment in Equation 2.6 mean, that if the plastic volumetric strain is negative, it is taken as zero. This ensures that the model predictions are sensible on the dry side of critical state, i.e. when $d\varepsilon_v^p<0$ and $\eta>M$, as well, even though this model is neither meant to be used nor is very accurate in such cases. The modulus symbol on the plastic deviatoric strain increment ensures that the value of α is dragged towards its target value despite the sign of the plastic deviatoric strain increment.

Plastic strains are calculated based on elasto-plastic theory as

$$d\varepsilon_v^p = \Lambda \frac{\partial g}{\partial p'} \tag{2.9}$$

$$d\varepsilon_d^p = \Lambda \frac{\partial g}{\partial q} \tag{2.10}$$

where Λ is the plastic multiplier and g is the plastic potential function. In S-CLAY1, flow rule is assumed to be associated, which means that the strain increment vectors are orthogonal to the plastic potential curve in p': q plane and the plastic potential function is equal to the yield function (g=f). Hence, based on the flow rule:

$$\frac{d\varepsilon_d^p}{d\varepsilon_v^p} = \frac{2(\eta-\alpha)}{M^2-\eta^2} \tag{2.11}$$

The consistency condition

$$df = 0 \tag{2.12}$$

gives

$$\frac{\partial f}{\partial p'}dp' + \frac{\partial f}{\partial q}dq + \frac{\partial f}{\partial p'_m}dp'_m + \frac{\partial f}{\partial \alpha}d\alpha = 0 \tag{2.13}$$

By combining Equations (2.5), (2.6), (2.9), (2.10) and (2.13) we obtain

$$\Lambda = \frac{\frac{\partial f}{\partial p'}dp' + \frac{\partial f}{\partial q}dq}{H} \tag{2.14}$$

where the hardening modulus H is defined as

$$H = -\left[\frac{\partial f}{\partial p'_m}\frac{\partial p'_m}{\partial \varepsilon_v^p}\frac{\partial f}{\partial p'} + \frac{\partial f}{\partial \alpha}\left(\frac{\partial \alpha}{\partial \varepsilon_v^p}\left\langle\frac{\partial f}{\partial p'}\right\rangle + \frac{\partial \alpha}{\partial \varepsilon_d^p}\left|\frac{\partial f}{\partial q}\right|\right)\right] \tag{2.15}$$

The partial derivatives required for Equation (2.15) are

$$\frac{\partial f}{\partial p'} = p'(\mathrm{M}^2 - \eta^2)\,^{1} \tag{2.16}$$

$$\frac{\partial f}{\partial q} = 2p'(\eta - \alpha) \tag{2.17}$$

$$\frac{\partial f}{\partial p'_m} = -p'(\mathrm{M}^2 - \alpha^2) \tag{2.18}$$

$$\frac{\partial p'_m}{\partial \varepsilon_v^p} = \frac{v p'_m}{\lambda - \kappa} \tag{2.19}$$

$$\frac{\partial f}{\partial \alpha} = 2p'(\alpha p'_m - q) \tag{2.20}$$

$$\frac{\partial \alpha}{\partial \varepsilon_v^p} = \mu\left(\frac{3\eta}{4} - \alpha\right) \tag{2.21}$$

---

[1] Assuming that the stresses stay at the yield surface.

$$\frac{\partial \alpha}{\partial \varepsilon_d^p} = \mu\beta\left(\frac{\eta}{3} - \alpha\right) \tag{2.22}$$

Now, by using the definition of hardening modulus H in Equation (2.15) in the case of associated flow rule, the stress-strain relationship can be expressed by the plastic compliance matrix:

$$\begin{bmatrix} d\varepsilon_v^p \\ d\varepsilon_d^p \end{bmatrix} = \frac{1}{H}\begin{bmatrix} \frac{\partial f}{\partial p'}\frac{\partial f}{\partial p'} & \frac{\partial f}{\partial q}\frac{\partial f}{\partial p'} \\ \frac{\partial f}{\partial p'}\frac{\partial f}{\partial q} & \frac{\partial f}{\partial q}\frac{\partial f}{\partial q} \end{bmatrix}\begin{bmatrix} dp' \\ dq \end{bmatrix} \tag{2.23}$$

2.3 Parameter determination

There are seven parameters in S-CLAY1. Five of them are the same soil constants as in Modified Cam Clay: λ, κ, M, G' or ν', and v or Γ. These can be determined from conventional laboratory tests. In addition, two new soil constants, namely μ and β are required. Determination of the values of these new soil constants will be discussed later on in this section. The initial state, i.e. initial inclination of the yield surface, α, and the initial size of the yield curve, p'_m, can be determined based on rather standard procedures in laboratory as will be shown next.

2.3.1 Initial inclination of yield surface

If the loading history of the normally or lightly overconsolidated soil deposit is one-dimensional K_0 loading, there is a fairly simple method for evaluating the initial value of α (Näätänen et al. 1999). Primarily, the value of the critical state parameter M is needed from triaxial test data. Then, in triaxial compression the value of the friction angle can be related to it via

$$\sin\varphi' = \frac{3M}{6+M} \tag{2.24}$$

In the case of one-dimensional loading history the coefficient of earth pressure at rest, K_0, can be estimated from Jaky's simplified formula (2.25), which is applicable for normally consolidated soils. Mayne and Kulhawy's (1982) formula (2.26) can be used to estimate the in situ K_0 in lightly overconsolidated soils.

$$K_0 = K_{0(NC)} \approx 1 - \sin\varphi' \tag{2.25}$$

$$K_0 = K_{0(OC)} \approx (1 - \sin\varphi') \cdot OCR^{\sin\varphi'} \tag{2.26}$$

The orientation of the yield curve can be assumed to have been created by normally consolidated K_0 loading. Hence, the corresponding value of η_{K0} can then be calculated from the $K_{0(NC)}$ as

$$\eta_{K0} = \frac{3(1 - K_{0(NC)})}{1 + 2K_{0(NC)}} \tag{2.27}$$

If elastic strains can be assumed much smaller than plastic strains, one-dimensional straining corresponds to

$$\frac{d\varepsilon_d^p}{d\varepsilon_v^p} = \frac{2}{3} \tag{2.28}$$

Combining Equation (2.28) and the flow rule in Equation (2.11), the initial inclination of the yield curve (Näätänen et al. 1999) becomes

$$\alpha_{K0} = \frac{\eta_{K0}^2 + 3\eta_{K0} - M^2}{3} \tag{2.29}$$

Therefore, the initial inclination of the yield curve is simply a function of the friction angle.

2.3.2 Initial size of yield curve

The value of p'_m can be calculated from Equation (2.4), if values of M and α and one point from the yield curve are known. This one yield point can be determined for instance from an isotropic or K_0-consolidation test in triaxial apparatus or from an oedometer test. Another way to determine p'_m is to fit the yield curve to a set of observations, when sufficient data is available. In this work the latter procedure is used.

2.3.3 Soil constant β

The soil constant β defines the relative effectiveness of plastic shear strains and plastic volumetric strains in rotating the yield curve. In the case of plastic loading along any constant η loading path, α eventually reaches an equilibrium value. According to Näätänen et al. (1999), this value can be calculated by setting $d\alpha=0$ in Equation (2.6) and combining it with Equation (2.11) that was used on the flow rule. This leads to

$$\left(\frac{3\eta}{4}-\alpha\right)\left(M^2-\eta^2\right)=\mp 2\beta\left(\frac{\eta}{3}-\alpha\right)(\eta-\alpha) \tag{2.30}$$

Näätänen et al. (1999) suggest, that the value of β at K_0 consolidation can then be calculated by combining Equations (2.29) and (2.30).

$$\beta=\frac{3\left(4M^2-4\eta_{K0}^2-3\eta_{K0}\right)}{8\left(\eta_{K0}^2-M^2+2\eta_{K0}\right)} \tag{2.31}$$

Hence, the value of β can also be estimated from the value of friction angle.

2.3.4 Soil constant μ

During loading parameter α tends towards its current target value, which depends on the stress path. The constant μ controls the rate of this rotation. According to Näätänen et al. (1999) there is no simple and direct method for determining μ experimentally, and

therefore there are two ways for resolving the problem. Where possible, it would be appropriate to carry out model simulations for several different values of μ, and then compare these with observed behaviour of soil. If it is not possible or practically feasible to carry out such a testing programme in required extent, an option is to select a standard default value for μ. Näätänen et al. suggested a value $\mu=20$ on the basis of the test data from Otaniemi clay.

3. MODEL COMBINING ANISOTROPY AND DE-STRUCTURATION (SS-CLAY1)

3.1 Background

In natural soft soils, there is often a degree of structure present in the soil. The term structure is used to mean the combination of fabric and interparticle bonding. Arrangement of particles is referred to as soil fabric. The anisotropy, discussed earlier, is a demonstration of the fabric arrangement. Structure develops during time because of various reasons, and it increases the strength of the soil compared to an unstructured soil.

Under loading conditions inside the yield curve the deformations that take place are elastic and when the yield stresses are exceeded, deformations become large and irrecoverable, i.e. plastic. Because of plastic deformations, some irrecoverable slipping starts to happen between the clay mineral platelets. All the platelets do not slip at the same time, but eventually under continued loading all of the structure of clay disappears. This means that in an isotropic triaxial test natural material has a compression line that curves towards the intrinsic compression line, and the slope of the curve tends towards the intrinsic value of λ. This is indicated in Figure 3.1.

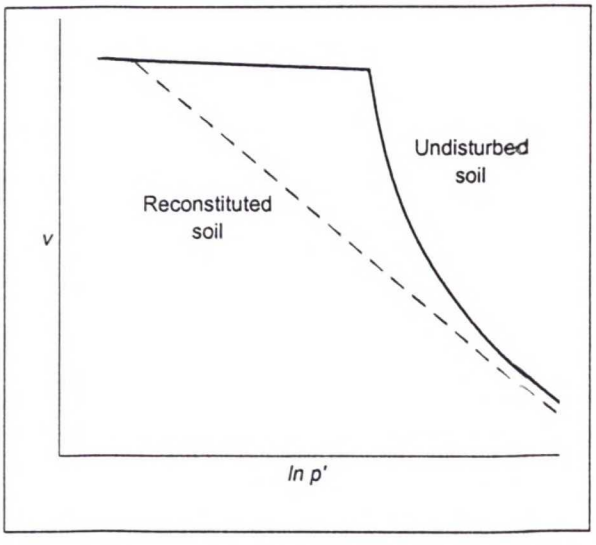

Figure 3.1. *Behaviour of reconstituted and undisturbed soil.*

Because of the effect of structure, supplementary component in describing the behaviour of soil is needed. This matter is handled by combining a feature that represents the bonding in the soil with S-CLAY1. This model, called SS-CLAY1, was suggested by Wheeler (2000) and initially applied by McGovern (2000). Properties of de-structured soil are called intrinsic in order to distinguish them from the properties of natural soil.

The basic ideas on elasto-plastic constitutive modelling of de-structuration were proposed by Gens and Nova (1993). However, they used an isotropic model to describe the fabric of the soil.

3.2 Model formulation

In SS-CLAY1, the form of the yield curve is identical to the yield curve of S-CLAY1. The yield curve of natural material is defined by Equation (2.4).

$$f = (q - \alpha p')^2 - (M^2 - \alpha^2)(p'_m - p')p' = 0 \qquad \text{(2.4 bis)}$$

Now, when soil with no structure is loaded, the yielding happens prior to the yield point of structured soil, as presented in Figure 3.1, because structure gives the soil extra strength. Therefore, the yield surface of an unstructured soil is smaller, and, for simplicity, it can be assumed to have the same shape than the yield curve of a natural soil and it is defined by Equation 2.4 s well. This curve is totally imaginary because in the ground structure always develops to some extent and cannot be removed without removing the stress history as well. The unstructured yield curve is called intrinsic yield curve and its size is p'_{mi}.

The difference between the sizes p'_m and p'_{mi} of the natural and unstructured yield curves describes the magnitude of bonding between the clay particles. That is described by a new parameter x so that the relationship between p'_m and p'_{mi} is

$$p'_m = (1 + x)p'_{mi} \qquad (3.1)$$

Situation is illustrated in Figure 3.2.

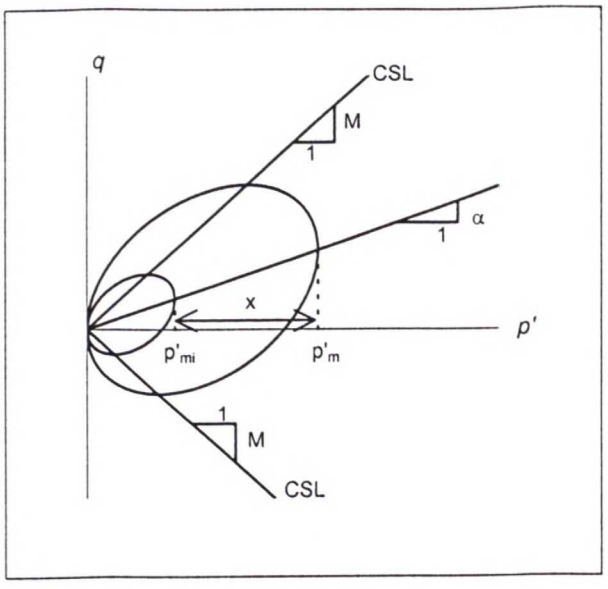

Figure 3.2. *Yield curves of intrinsic material and natural material.*

Elastic behaviour inside the yield surface is described as isotropic with the same elastic relationship as in S-CLAY1 and Modified Cam Clay.

$$\begin{bmatrix} d\varepsilon^e_v \\ d\varepsilon^e_d \end{bmatrix} = \begin{bmatrix} \frac{\kappa}{vp'} & 0 \\ 0 & \frac{1}{3G'} \end{bmatrix} \begin{bmatrix} dp' \\ dq \end{bmatrix} \qquad (2.1 \text{ bis})$$

The hardening laws that control the changes in the size of the intrinsic yield curve and the inclination of both yield curves are formally the same as in S-CLAY1.

$$dp'_{mi} = \frac{vp'_{mi}}{\lambda - \kappa} d\varepsilon^p_v \qquad (3.2)$$

$$d\alpha = \mu \left[\left(\frac{3\eta}{4} - \alpha \right) \left\langle d\varepsilon^p_v \right\rangle + \beta \left(\frac{\eta}{3} - \alpha \right) \left| d\varepsilon^p_d \right| \right] \qquad (3.3)$$

The hardening law that controls the degradation of the bonding effect is similar in principle to Equation (3.3) and it can be presented with Equation (3.4). The target value of bonding parameter x is zero, since the structure tends to be completely destroyed, and hence Equation (3.4) can be simplified to the latter form.

$$dx = a\left[(0-x)\left|d\varepsilon^{p}_{v}\right| + b(0-x)\left|d\varepsilon^{p}_{d}\right|\right] = -ax\left(\left|d\varepsilon^{p}_{v}\right| + b\left|d\varepsilon^{p}_{d}\right|\right) \tag{3.4}$$

Parameters a and b in Equation (3.4) are new soil constants, that control the absolute rate at which de-structuration takes place in the soil and the effectiveness of the plastic deviatoric strains in relation to the plastic volumetric strains in destroying the structure.

The hardening law describing the changes in size of the structured yield curve can be expressed based on Equation (3.1) as

$$dp'_{m} = (1 + x + dx)(p'_{mi} + dp'_{mi}) - (1 + x)p'_{mi} \tag{3.5}$$

By simplifying, we obtain

$$dp'_{m} = p'_{mi}\,dx + dp'_{mi}\,(1 + x + dx) \tag{3.6}$$

Again, an associated flow rule is assumed and hence

$$\frac{d\varepsilon^{p}_{d}}{d\varepsilon^{p}_{v}} = \frac{2(\eta - \alpha)}{M^{2} - \eta^{2}} \tag{2.11 bis}$$

The consistency condition for the SS-CLAY1 can be expressed as

$$\frac{\partial f}{\partial p'}dp' + \frac{\partial f}{\partial q}dq + \frac{\partial f}{\partial p'_{mi}}dp'_{mi} + \frac{\partial f}{\partial x}dx + \frac{\partial f}{\partial \alpha}d\alpha = 0 \tag{3.7}$$

Again, based on standard elasto-plastic procedure

$$\Lambda = \frac{\frac{\partial f}{\partial p'}dp' + \frac{\partial f}{\partial q}dq}{H} \tag{3.8}$$

where the hardening modulus is now

$$H = -\left[\frac{\partial f}{\partial p'_{mi}}\frac{\partial p'_{mi}}{\partial \varepsilon^{p}_{v}}\frac{\partial f}{\partial p'} + \frac{\partial f}{\partial x}\left(\frac{\partial x}{\partial \varepsilon^{p}_{v}}\left|\frac{\partial f}{\partial p'}\right| + \frac{\partial x}{\partial \varepsilon^{p}_{d}}\left|\frac{\partial f}{\partial q}\right|\right) + \frac{\partial f}{\partial \alpha}\left(\frac{\partial \alpha}{\partial \varepsilon^{p}_{v}}\left\langle\frac{\partial f}{\partial p'}\right\rangle + \frac{\partial \alpha}{\partial \varepsilon^{p}_{d}}\left|\frac{\partial f}{\partial q}\right|\right)\right] \tag{3.9}$$

The additional partial derivatives required for Equation (3.9) are

$$\frac{\partial f}{\partial p'_{mi}} = -p'(1+x)(\mathrm{M}^2 - \alpha^2) \tag{3.10}$$

$$\frac{\partial p'_{mi}}{\partial \varepsilon_v^p} = \frac{v}{\lambda - \kappa} p'_{mi} \tag{3.11}$$

$$\frac{\partial f}{\partial \alpha} = 2p'\left[(1+x)p'_{mi}\,\alpha - q\right] \tag{3.12}$$

$$\frac{\partial f}{\partial x} = -p'\,p'_{mi}\,(\mathrm{M}^2 - \alpha^2) \tag{3.13}$$

$$\frac{\partial x}{\partial \varepsilon_v^p} = -ax \tag{3.14}$$

$$\frac{\partial x}{\partial \varepsilon_d^p} = -axb \tag{3.15}$$

Hence, the plastic compliance matrix is again

$$\begin{bmatrix} d\varepsilon_v^p \\ d\varepsilon_d^p \end{bmatrix} = \frac{1}{H}\begin{bmatrix} \frac{\partial f}{\partial p'}\frac{\partial f}{\partial p'} & \frac{\partial f}{\partial q}\frac{\partial f}{\partial p'} \\ \frac{\partial f}{\partial p'}\frac{\partial f}{\partial q} & \frac{\partial f}{\partial q}\frac{\partial f}{\partial q} \end{bmatrix}\begin{bmatrix} dp' \\ dq \end{bmatrix} \tag{2.23 bis}$$

3.3 Parameter determination

There are three extra parameters in the combined model SS-CLAY1 compared to the anisotropic model S-CLAY1. These are the rate parameters a and b, and parameter x that describes the effect of structure in terms of the apparent size of the yield curve. Values of a and b are determined in this case from simulations that are done for a few different values and then compared with observed behaviour of natural clays. Parameter x is estimated initially on the basis of the sensitivity of natural clays considered.

The parameter λ differs in case of combined model SS-CLAY1 from the parameter used in case of S-CLAY1. In this case, the λ-value for unstructured soil ($\lambda_{intrinsic}$) is required, and it is determined based on laboratory tests on reconstituted samples as presented in Chapter 4. All other model parameters are the same as in S-CLAY1 and their determination was discussed in Chapter 2.

4. EXPERIMENTAL TESTS

In order to test the model SS-CLAY1, in which both anisotropy and de-structuration are combined, laboratory tests on samples with and without structure, i.e. natural and reconstituted samples, were required. Two different soft soils were used as testing material: a silty clay from Bothkennar test site for developing the laboratory technique and a soft clay from Finland called POKO clay for substantial testing. The structured soil samples that were used were natural, undisturbed soil samples and the unstructured soil samples were prepared by remoulding the natural soil. Burland (1990) suggested, that a sample without structure could be prepared by reconstituting: i.e. remoulding natural soil in water content between $w_L \ldots 1{,}5w_L$ (w_L is the liquid limit) without drying the soil first. Properties of reconstituted soil are called intrinsic properties.

After reconstituting, there may be still some negligible bonding left in the soil and it is assumed to be of electrostatic or electromagnetic by nature.

4.1 Bothkennar clay

4.1.1 Properties of Bothkennar clay

Bothkennar is a soft clay test site in Scotland situated in Grangemouth area between Glasgow and Edinburgh. The site is located on the bank of Forth Estuary. The site area is 11 ha and flood embankments bound it on three sides. Bothkennar clay is very uniform compared to other British clays.

The total thickness of the clay deposit is more than ten meters. Bothkennar clay is normally consolidated or lightly overconsolidated post-glacial silty clay and the main minerals are quartz, illite and chlorite (Paul et al. 1992). Some index properties of Bothkennar clay are presented in Table 4.1 (McGinty 2000).

Table 4.1. *Index properties of Bothkennar clay.*

z	11.2-11.4 m
w	57 %
w_L	62 %
γ	17 kN/m^3
G_s	2.68

4.1.2 Experimental procedure and equipment

The samples that were used in experiments were taken with a Laval sampler in 1989 and stored in a cool and moist atmosphere until they were used. Because sampling was done over 10 years ago there was a shortage of material. Hence, natural soil was not used for preparing the reconstituted samples. Natural soil was tested first as undisturbed samples and then dried in the oven and used again for reconstituting.

Reconstituted samples for triaxial tests were made of Bothkennar clay powder and de-aired tap water. Powder was mixed together with the water by hand so that the slurry was liquid enough to be poured easily into a Perspex cylinder with a 38 mm diameter. Water content (w) of the slurry was more than the liquid limit w_L=62 % of Bothkennar clay. Because of the natural variation between samples, the water content needed for achieving good slurry varied, and water contents between 70 % and 124 % were used.

On the bottom of the Perspex cylinder there was a piston, a porous stone and one or two layers of filter paper. Filter paper was needed in the interface of the slurry and the porous stones to prevent clay particles from escaping from the cylinder and blocking the porous stone. Porous stones were boiled in de-aired water at least for 30 minutes so that they were fully saturated. Above the slurry there were also one or two layers of filter paper, a porous stone and a piston. After fitting the latter ones the sample was consolidated one-dimensionally in a frame, which gave a load of 76 N (67 kPa). Additional dead-weight load was added in approximately an hour, if necessary. The actual stress due to the load varied with the friction between Perspex cylinder and filter papers. Frame and loading arrangements are presented in Figure 4.1.

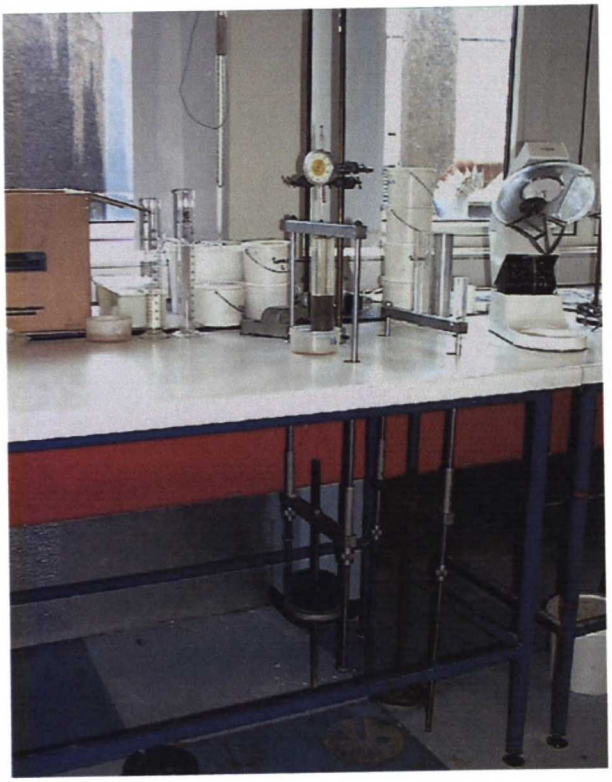

Figure 4.1. *Loading arrangements of one-dimensional consolidation in Perspex cylinder.*

Drainage during consolidation was allowed from both ends of the sample. Drained water was noticed to be yellow or brown, and after that water had evaporated, some sort of crystals remained on the bottom of the bowl.

Because soil was fully saturated, initial void ratio could be calculated from

$$e_0 = wG_s \tag{4.1}$$

where G_s is the specific density of soil, in this case 2.68. Because soil particles are incompressible, the height of soil particles H_s was constant and the final void ratio after consolidation could be determined from

$$e_f = \frac{H_f}{H_s} - 1 \tag{4.2}$$

where

$$H_s = \frac{H_i}{1+e_0} \tag{4.3}$$

Initial height of the slurry $H_i \approx 10$ cm gave after loading approximately the final height $H_f \approx 7.6$ cm as required for the triaxial testing, so trimming the sample could be avoided as well as disturbance caused by trimming. The stress state in the ends of the sample was not the same as in the middle of the sample due to the distribution of stresses due to consolidation and non-uniform friction.

Reconstituted samples of Bothkennar clay were after one-dimensional consolidation extruded from the Perspex cylinder and consolidated isotropically in conventional triaxial cell to same known stress-state by applying change of cell-pressure as step loading. After isotropic consolidation samples were unloaded to different values of mean effective stress and then sheared using a path with a slope of 3:1, i.e. keeping the cell pressure constant.

Samples were placed in triaxial cell so that drainage was possible from both ends as well as from the radial boundary. Drainage was possible against a back pressure of 100 kPa, which was applied in each test in order to make sure that possible little amounts of air in pores of the samples remained in solution. During the tests change of volume, cell pressure, back pressure, deviator force and axial strains were measured and logged in by a computer.

To be sure that in each step of isotropic consolidation primary consolidation had ended, change of volume was plotted against logarithm of time or square root of time and analysed with Taylor and Casagrande methods.

Test series included three isotropic consolidation and shearing tests. Information about those tests can be seen in Table 4.2.

Table 4.2. *Bothkennar clay test series on reconstituted samples.*

Test number	p'_{Imax} *kPa*	$p'_{unloading}$ *kPa*
CID 1	295	233
CID 2	312	115
CID 3	295	176

4.1.3 Experimental results

The main purpose of the test programme of Bothkennar clay was to practise the testing technique. In addition, an objective was to study the difference between the values of λ for structured and de-structured soil. Another objective was to examine, if de-structuration has an effect on the value of the critical state parameter M.

Stress paths used in testing are presented in Figure 4.2 and included are the yield points from the shearing phase as well. The yield curve in Figure 4.2 has been drawn assuming that the sample is isotropic after consolidation to the maximum value of mean effective stress. The yield points interpreted support this assumption fairly well.

The values of λ, κ and M were determined from each test as well. Those results as well as the yield points are presented in Table 4.3. Also presented are the corresponding values from an isotropic, natural, undisturbed test CAD 11 (McGinty, 2000). Yield points are determined as cross points of normal consolidation line and overconsolidation line from ln p': v plots.

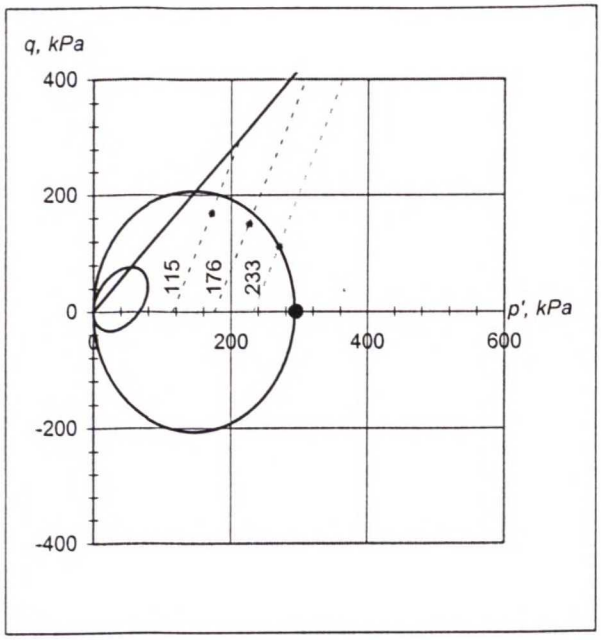

Figure 4.2. *Stress paths and yield points in tests on reconstituted Bothkennar clay.*

Table 4.3. *Yield points and the values of parameters λ, κ and M of Bothkennar clay.*

Test number	*λ*	*κ*	*M*	*p_y'*	*q_y*	*Sample*
CID 1	0.151	0.05	1.43	270	111	Reconstituted
CID 2	0.161	0.031	1.40	171	168	Reconstituted
CID 3	0.157	0.05	-	226	150	Reconstituted
CAD 11	0.337	0.031	-	-	-	Undisturbed

It can be seen from the results, that the value of λ is considerably smaller in tests performed for reconstituted samples, but as for the values of κ, there is no significant difference. According to McGinty (2000) the value of M for natural samples is 1.4, so there is no effect of structure on the value.

4.2 POKO clay

4.2.1 Properties of POKO clay

POKO clay from southern Finland near city of Porvoo was chosen for the main testing material. It was chosen because of its availability and because its initial yield surface had already been determined by Näätänen & Lojander (2000).

The groundwater level is about 0.9 m below the ground surface of the clay deposit. In Figure 4.3 is presented the grain size distribution of the material from the layer that is studied.

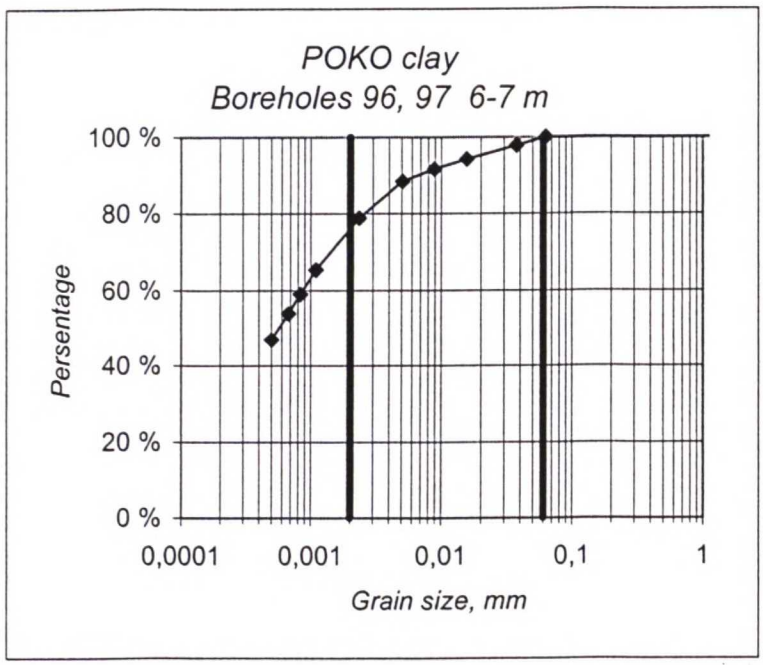

Figure 4.3. *Grain size distribution of POKO clay.*

Other index properties of POKO clay are presented in Figure 4.4, which incorporates the whole profile. The data used in profile are from two boreholes that are very similar. The borehole that has been studied in this work has been marked as number 97. In Figure 4.4 b) some scatter can be seen which is typical for Finnish clays due to the inhomogeneity.

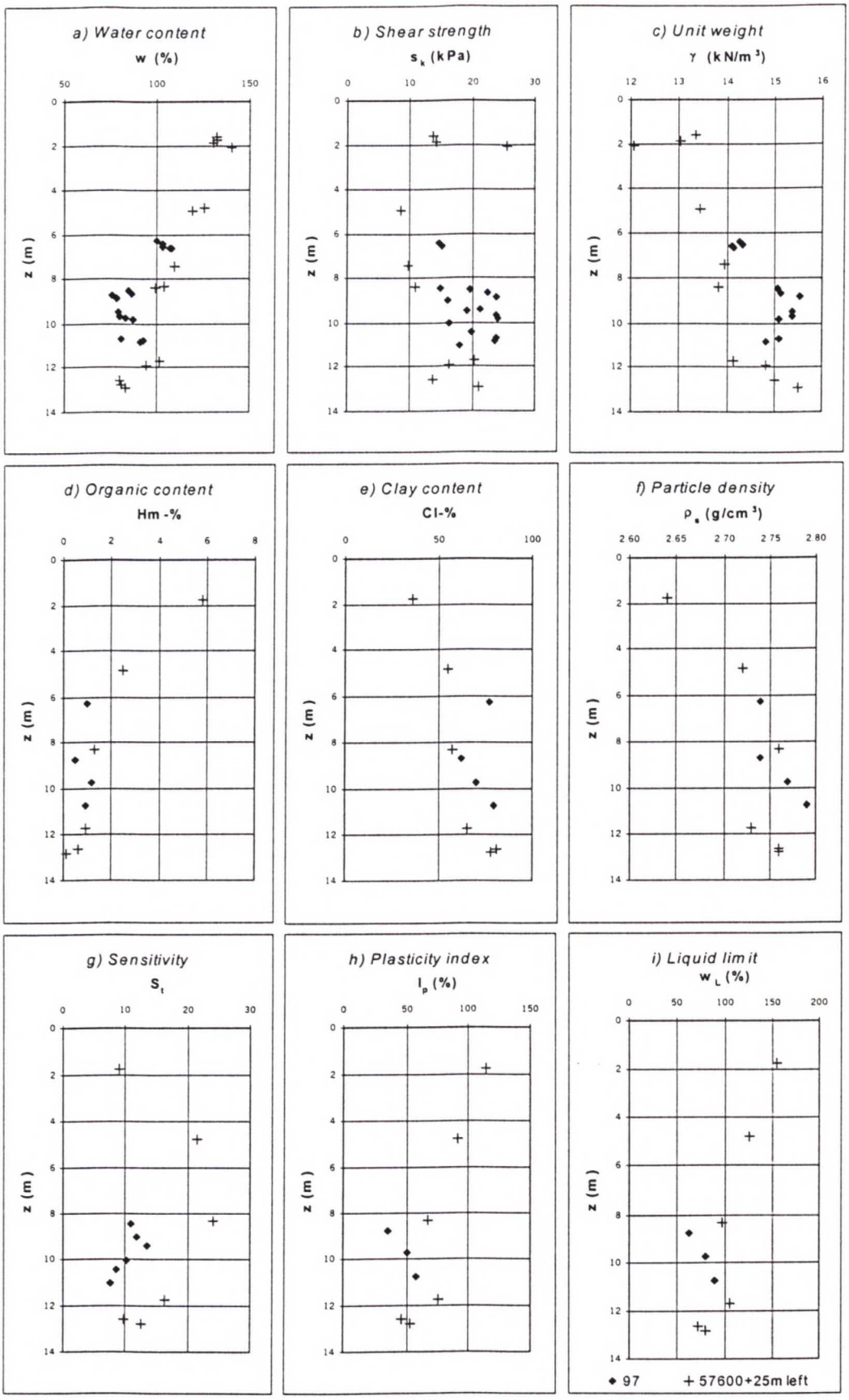

Figure 4.4. *Profile of POKO clay.*

4.2.2 Experimental procedure and equipment

For testing POKO clay, high quality undisturbed samples were used. Samples were from boreholes 96 and 97. For sampling, Swedish and Norwegian types piston samplers were used so that the diameter of the sample was either 50 mm or 54 mm depending on the type of the sampler. Test programme included tests on both undisturbed and reconstituted samples. Those were mainly triaxial consolidation tests, but some triaxial shear tests and oedometer tests were also carried out. Swedish type samples were used for undisturbed tests and Norwegian type samples were reconstituted. Undisturbed samples were trimmed only by cutting them to height of 100 mm for triaxial testing.

Samples were taken from two depths: undisturbed samples were from depth 8.5-11.0 m and reconstituted samples from depth 6-7 m. In spite of the difference between depths they are considered comparable on the basis of some essential index properties that are presented in Table 4.4.

Table 4.4. *Some index properties of POKO clay.*

	Depth 6-7 m	*Depth 8.5-11.0 m*
Clay content, %	77	62...79
Organic content, %	1	0.5...1.2
Particle density, g/cm^3	2.74	2.74...2.79
Water content, %	81...84	76...92

POKO clay was reconstituted for triaxial testing in the way proposed by Burland (1990): remoulding natural soil in water content that was higher than natural. This was done with an ordinary food mixer where distilled water was added to the clay slurry until it was in liquid form. The slurry was then poured in a Perspex cylinder between filter papers and porous stones, as was the case with Bothkennar clay samples. The dimensions of the Perspex cylinders differed from the ones used in Glasgow for Bothkennar clay. The diameter was 50 mm instead of 38 mm. Initial height of the slurry

in the beginning of the one-dimensional consolidation was considerably higher, approximately 18 cm.

Samples were then consolidated one-dimensionally in a loading frame. Vertical load was chosen smaller than for Bothkennar clay because of the differences between the compressibility and permeability properties of the clays studied. No additional dead weight loading was needed in addition to the 15 kPa load induced by the frame.

Loading time was chosen to be two weeks on the basis of the end of primary consolidation. This was verified with the square root of time fitting method from plots of change of height against square root of time (Atkinson 1995). This is illustrated in Figure 4.5.

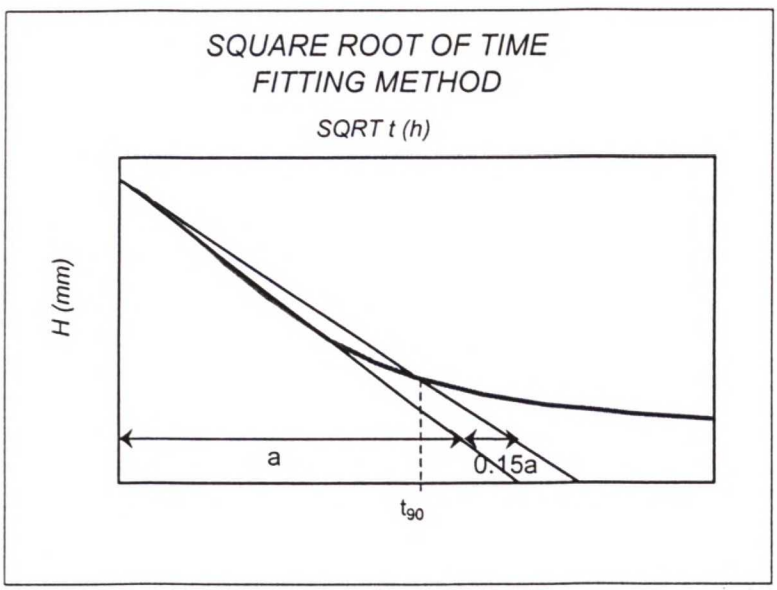

Figure 4.5. *Square root of time fitting method.*

After the one-dimensional consolidation, samples were extruded from the Perspex cylinders and tested immediately in triaxial apparatus with the usual practice in the Laboratory of Soil Mechanics at Helsinki University of Technology. This practice follows the international practice concerning triaxial testing (Berre 1995) and was implemented to all the tests, both on undisturbed and reconstituted samples, carried out for this testing programme.

Drainage was allowed from both ends and the radial boundary by equipping the sample with saturated porous stones on both ends and filter paper strips fitted to an angle of 45 degrees. The joints between the caps and the membrane were sealed with silicon and rubber rings in order to prevent any contact between the sample and the water in the cell. Pore pressure was not measured in consolidation tests and drained shearing tests, so the samples were able to drain from both ends.

Oedometer tests on natural samples were standard step-wise oedometer tests (Atkinson 1995). Oedometer tests on reconstituted samples were also done by using the same procedure, but testing material was clay remoulded in water content higher than natural.

The test programme itself included two series: first a triaxial test series for natural samples and second for reconstituted samples. In addition, some oedometer tests were carried out in order to get an idea if the values of λ determined from oedometer test correspond to the values determined from triaxial consolidation tests.

Summary of the undisturbed test series is presented in Table 4.5. The measured stress paths from each test are also included. All the tests included first and second loading. Stress paths in first and second loading were chosen to differ from one another considerably in order to show the rotation of the yield curve.

Table 4.5. *Tests on natural samples of POKO clay.*

Test number	*Borehole*	*Depth* *m*	η_1	η_2
CAD 2767	97	8.53-8.64	0.21	0.88
CAD 2751	97	8.73-8.83	0.95	0.055
CAD 2750	97	8.88-8.98	0.33	0.60
CAE 2737	97	9.53-9.64	0.59	-0.60
CAD 2736	97	9.70-9.81	0.07	-
CAE 2728	97	9.87-9.98	-0.60	0.60
CAE 2770	97	10.87-10.98	-0.22	0.55

The test series on reconstituted samples was planned to repeat some of the tests on undisturbed samples as can be seen in Table 4.6. First loading in each test was a loading that followed approximately the K_0 stress path, and second and third loadings followed the stress paths similar to the corresponding test on natural sample. In Table 4.6, the stress paths shown are the measured paths. Each of the tests took in between two to three months to carry out.

Table 4.6. *Tests on reconstituted samples of POKO clay.*

Test number	*Corresponding undisturbed test*	*Borehole*	*Depth m*	η_1	η_2	η_3
CAD 2854R	CAD 2767	96, 97	6-7	0.65	0.21	0.88
CAD 2855R	CAD 2751	96, 97	6-7	0.65	0.91	0.055
CAE 2856R	CAE 2737	96, 97	6-7	0.65	0.59	-0.60
CAE 2857R	CAE 2770	96, 97	6-7	0.65	-0.22	0.55

Oedometer test series included three undisturbed standard tests with cross loading steps so that they could be combined in a same figure for determining the λ value. In addition, one reconstituted oedometer test was carried out. The summary of oedometer tests is presented in Table 4.7.

Table 4.7. *Oedometer tests on POKO clay.*

Test number	*Borehole*	*Depth m*	*Sample*
2773	97	8.87-8.90	Undisturbed
2771	97	9.64-9.67	Undisturbed
2771	97	9.98-10.01	Undisturbed
2844uR	96, 97	6-7	Reconstituted

5. POKO CLAY TEST RESULTS AND SIMULATIONS

5.1 Test results of natural samples

5.1.1 Test results

In this section the results of tests on undisturbed POKO clay from the triaxial and oedometer test series that were introduced in Chapter 4 are presented. From each triaxial test two plots are shown: ln p': ε_V plot and ε_s: ε_V plot. These plots can be found in Figures from 5.1 to 5.7.

In the figures, different markers symbolize different loading stages. First loading and unloading are marked with a diamond and reloading and unloading are marked with a triangle. Open marker characterizes unloading. Strains are natural strains, and they are scaled to begin from the first step in which the stress ratio is constant. This principle is applied to all the figures in this chapter.

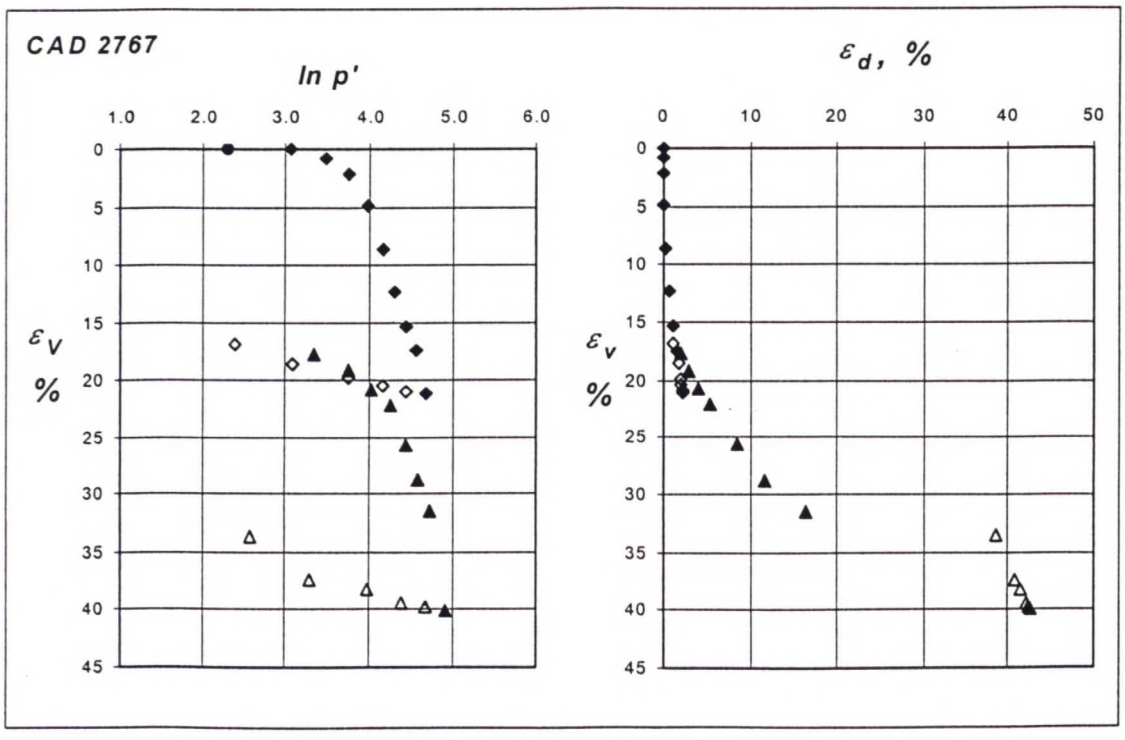

Figure 5.1. *Test CAD 2767 on natural POKO clay, η_1=0.21 and η_2=0.88.*

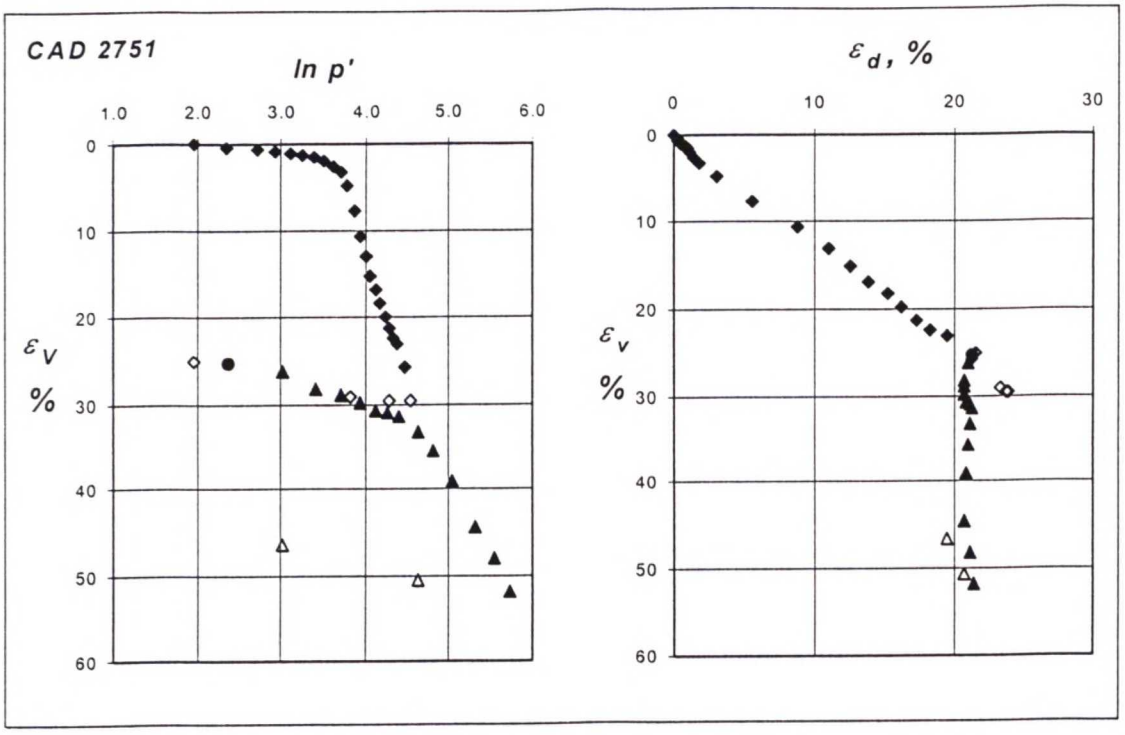

Figure 5.2. *Test CAD 2751 on natural POKO clay, η_1=0.95 and η_2=0.055.*

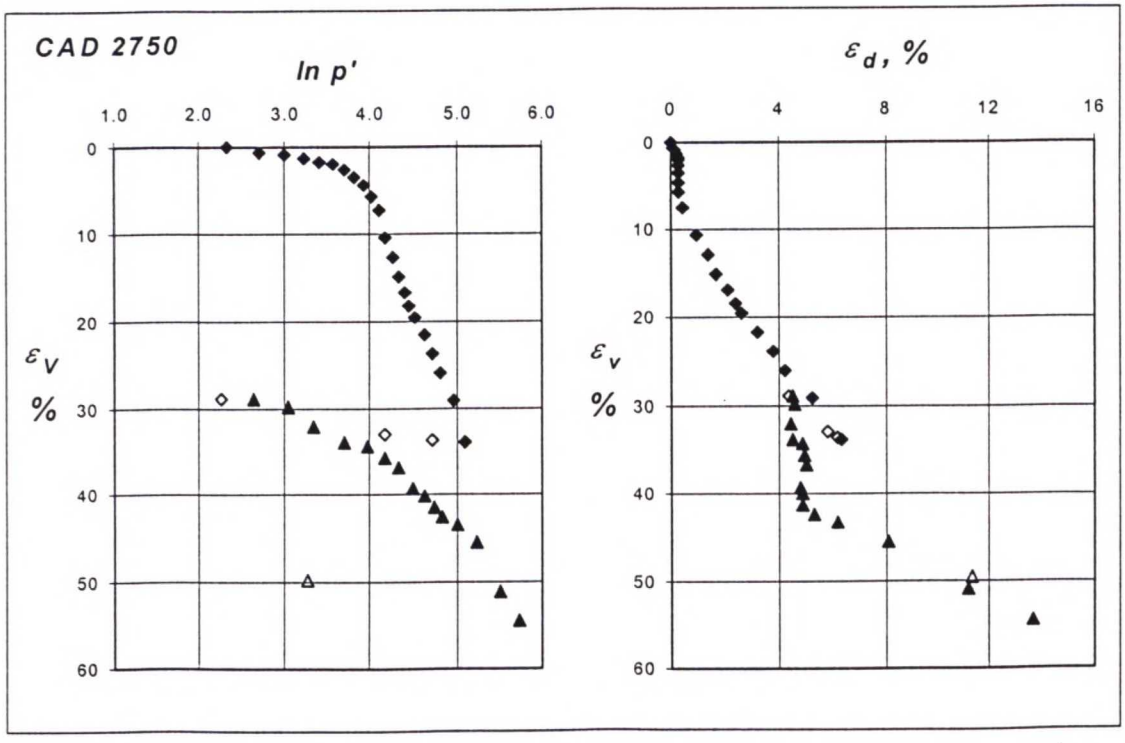

Figure 5.3. *Test CAD 2750 on natural POKO clay, η_1=0.33 and η_2=0.60.*

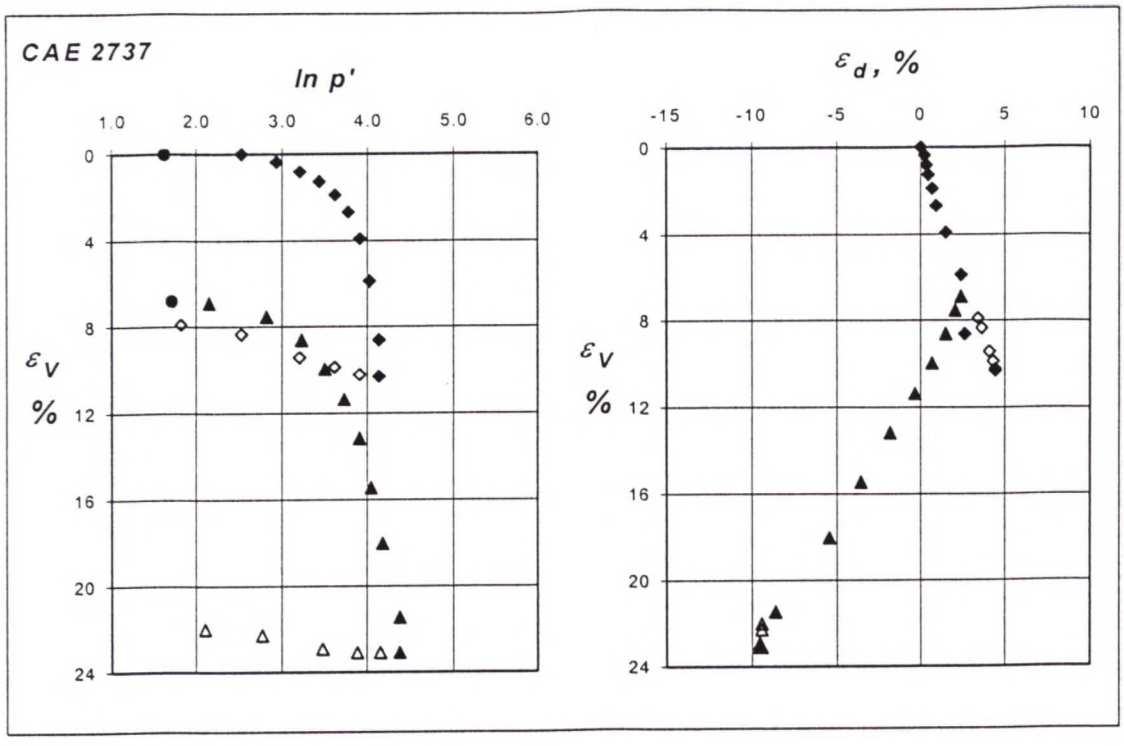

Figure 5.4. *Test CAE 2737 on natural POKO clay, η_1=0.59 and η_2=-0.60.*

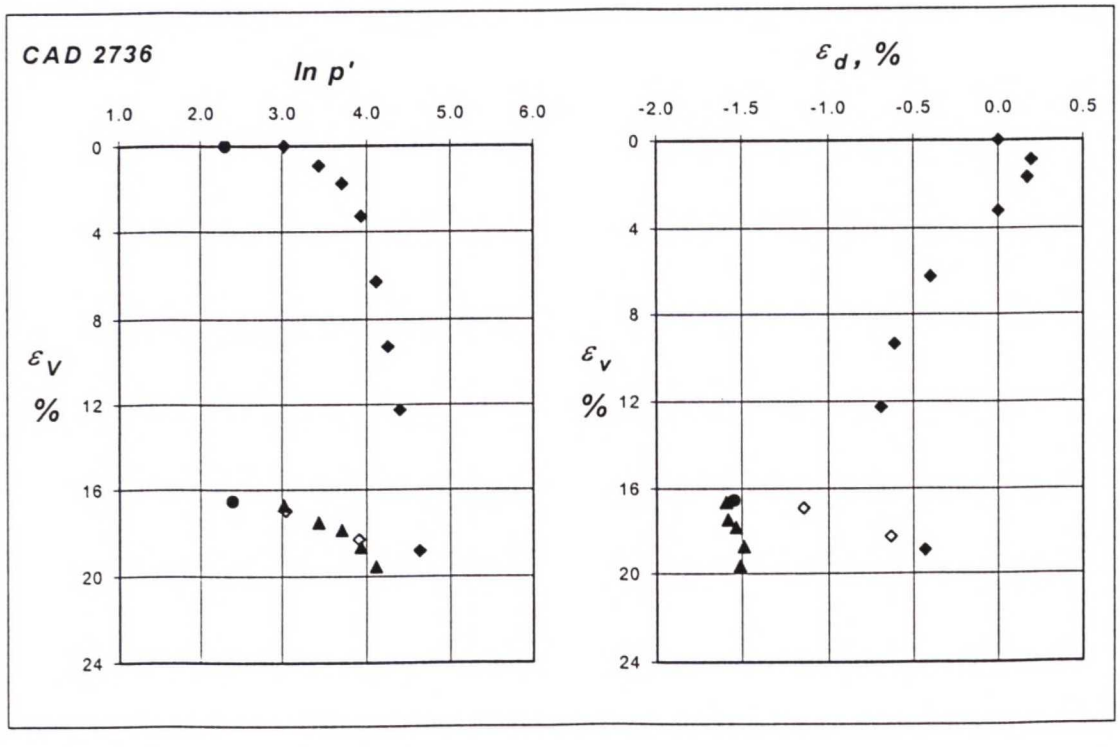

Figure 5.5. *Test CAD 2736 on natural POKO clay, η=0.07.*

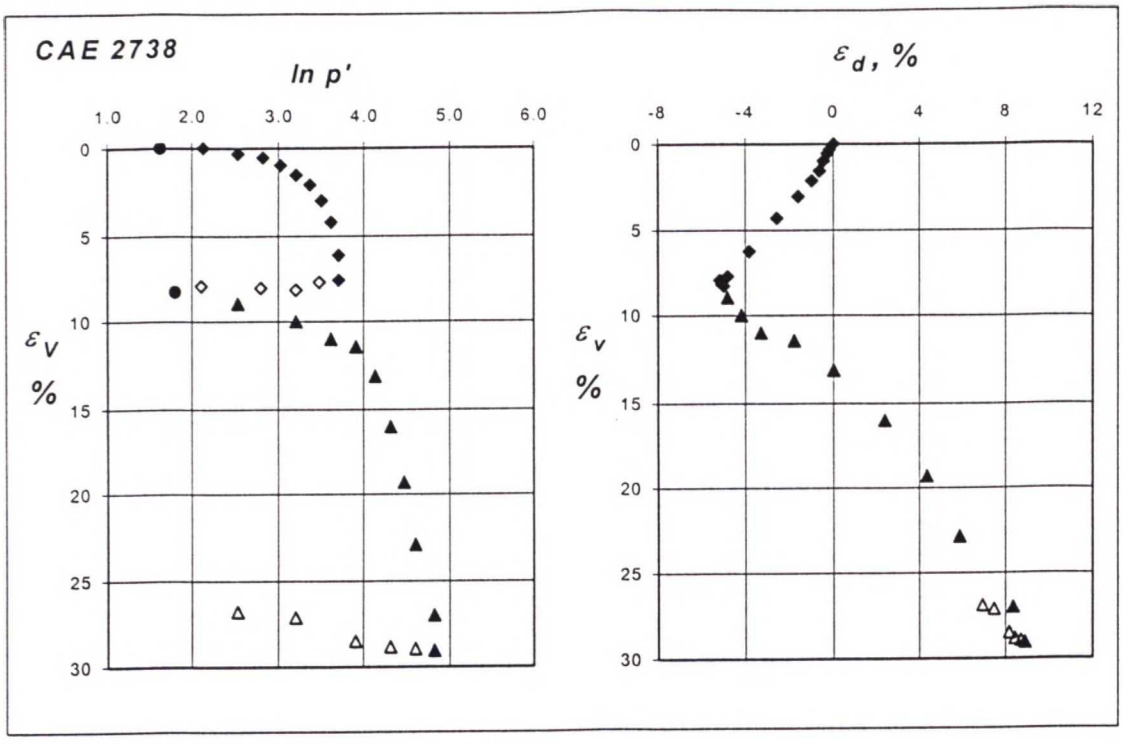

Figure 5.6. *Test CAE 2738 on natural POKO clay, η_1=-0.60 and η_2=0.60.*

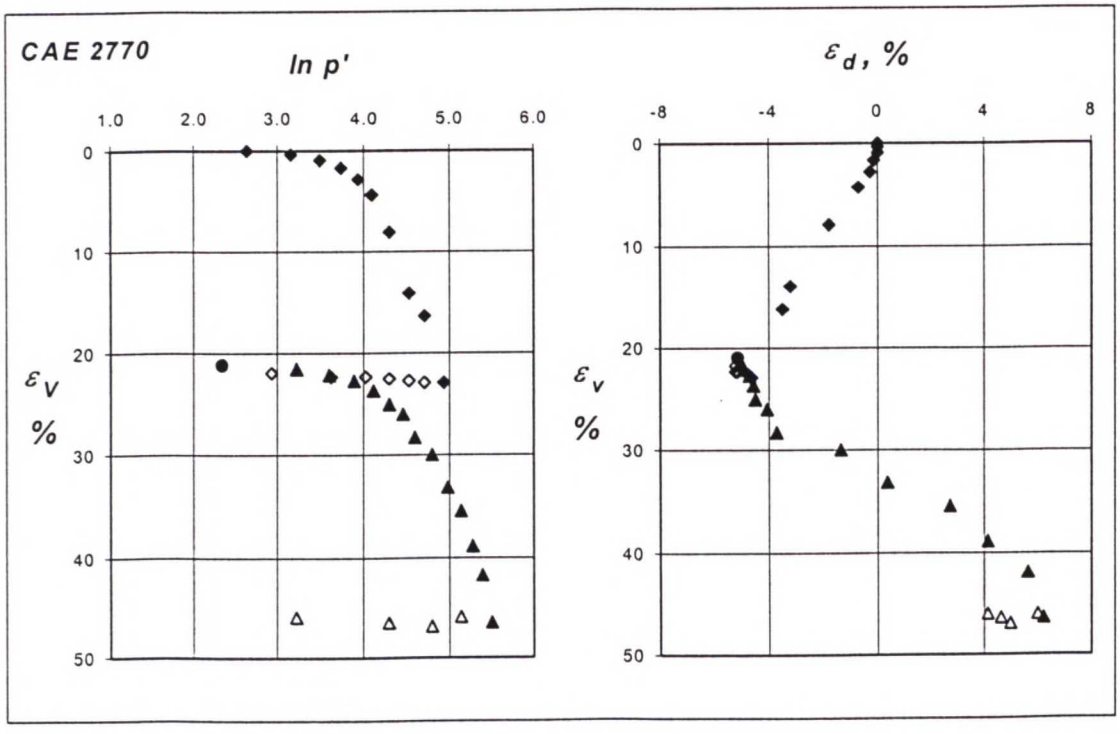

Figure 5.7. *Test CAE 2770 on natural POKO clay, η_1=-0.22 and η_2=0.55.*

Test CAD 2736 in Figure 5.5 included only one consolidation stage, and the sample was then sheared.

The three oedometer tests that were carried out can be drawn as a combined curve in terms of axial stress and axial strain. This is presented in Figure 5.8. Based on the results, the preconsolidation pressure σ_p can be estimated to be about 70 kPa.

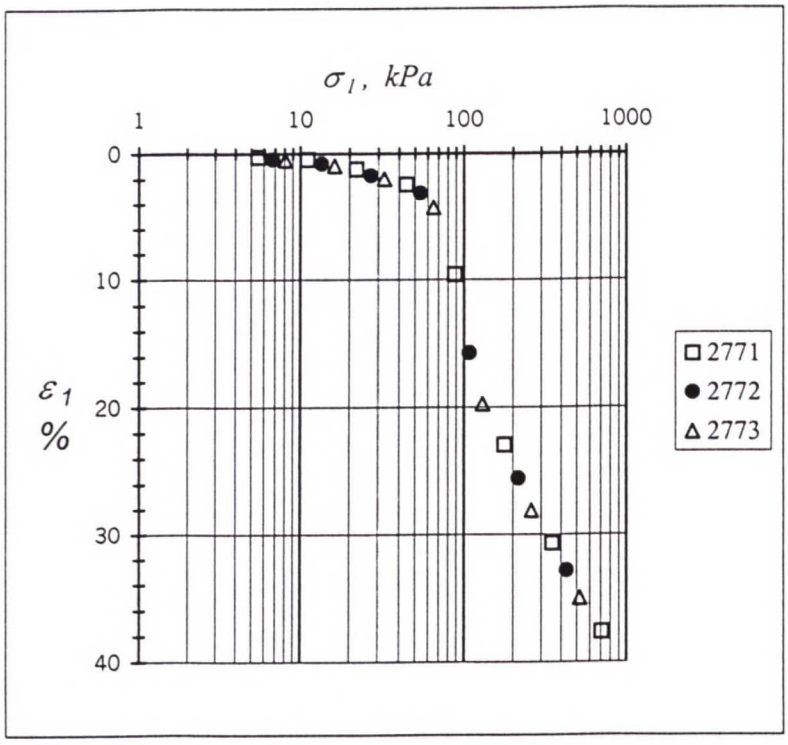

Figure 5.8. *Oedometer tests 2771 to 2773 on natural POKO clay.*

5.1.2 Parameters λ and κ

Based on the consolidation test results, yield points and values of parameters λ and κ were determined. The κ-line was fitted to either overconsolidation line of first loading or to unloading-reloading line depending on the amount of feasible points on them. Since the stress ratio varied slightly in the beginning of each loading stage, only the points with correct stress ratio were taken into account in deciding the value of κ.

This principle was applied to determining the values of parameter λ, as well. In addition, in defining λ steps that took more than one day were ignored. It was not

possible to keep the loading time constant because of weekends. The principle of determination of λ and κ is presented in Figure 5.9.

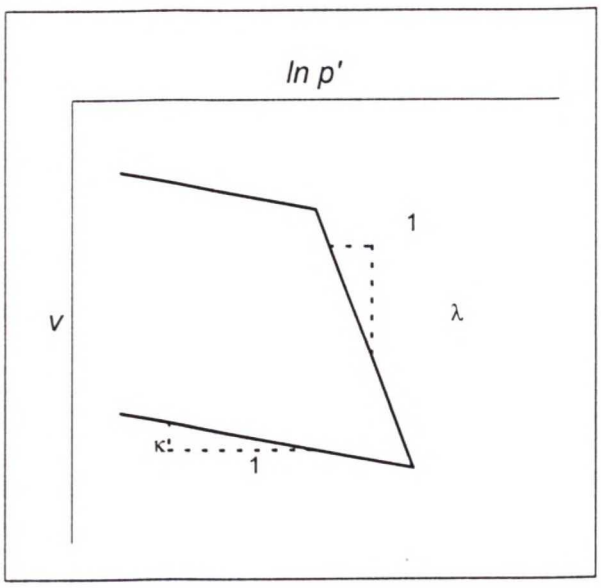

Figure 5.9. *Parameters λ and κ.*

The determined values of λ and κ are presented in Table 5.1. It can be seen that the dependence of κ on stress ratio is minor compared to that of λ. The higher is stress ratio, the higher is λ as well. This arises from the fact that the value of λ approaches its intrinsic value faster in tests where stress ratio is high, because this causes rapid de-structuring effect in the sample.

Table 5.1. *Values of λ and κ from tests on natural POKO clay.*

Test number	λ	κ	η_l
CAD 2767	0.604	0.024	0.21
CAD 2751	1.059	0.019	0.95
CAD 2750	0.738	0.020	0.33
CAE 2737	0.657	0.020	0.58
CAE 2736	0.607	0.021	0.07
CAE 2738	0.560	0.014	-0.60
CAE 2770	0.552	0.017	-0.22

It is possible to define the values of λ and κ with the same procedure from oedometer tests as well. Oedometer tests are easier and faster to carry out than triaxial tests and do not need as sophisticated equipment so it might be a reasonable practice to determine the λ value used in practical design indeed from oedometer test results.

The oedometer test series on POKO clay would suggest values λ=0.86 and κ=0.021. In Figure 5.10 it can be seen how well this value of λ corresponds to the values determined from triaxial tests in relation to the stress ratio η. In oedometer test the consolidation takes place at K_0 condition, because no radial deformations are possible. Therefore, the stress ratio in oedometer test stands for the η_{K0}=0.67 in triaxial test when the value of K_0 is estimated via Jaky's simplified formula.

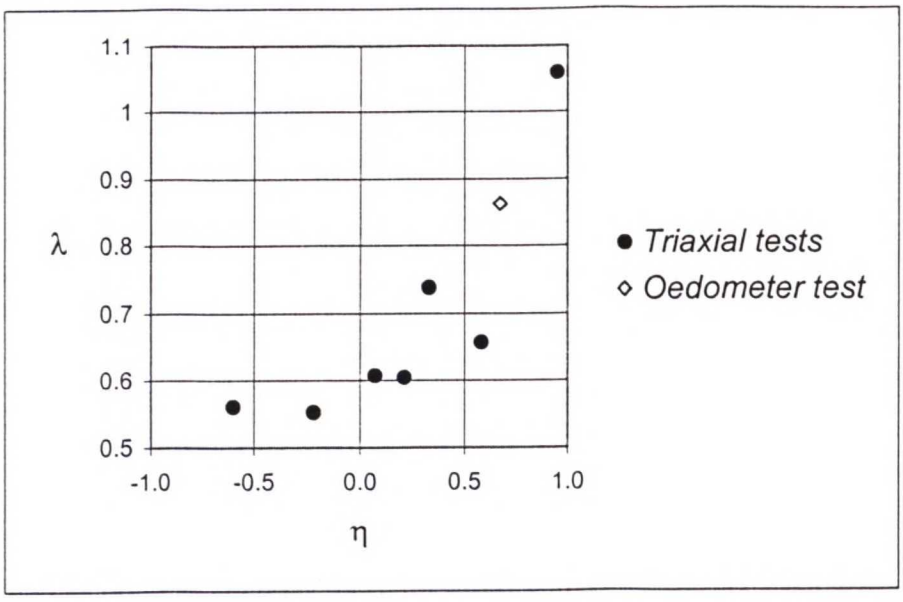

Figure 5.10. *Values of λ in relation to the stress ratio of POKO clay.*

It can be seen that λ from the oedometer test corresponds very well to the same increasing tendency with the values of λ from triaxial tests. It is noteworthy, that in order to gain a value of λ from oedometer test as accurately as possible, the loading steps should be added as quite small increments, and not double the load each step as is the standard practice.

5.1.3 Yield points

Yield points were defined as the intersection points of overconsolidation line and normal consolidation line in ln p': ε_v plots. Therefore, yield points were determined on the basis of λ lines of each test. The yield points are presented in Table 5.2.

Table 5.2. *Yield points of natural POKO clay.*

Test number	η_1	p'_{y1} *kPa*	q_{y1} *kPa*	p'_{1max} *kPa*	η_2	p'_{y2} *kPa*	q_{y2} *kPa*
CAD 2767	0.21	44.6	8.9	108	0.88	66.0	58.5
CAD 2751	0.95	40.4	38.7	93.1	0.055	70.1	3.8
CAD 2750	0.33	49.0	15.4	162	0.60	-	-
CAE 2737	0.59	43.5	25.3	62.2	-0.60	36.7	-21.8
CAE 2736	0.07	47.4	3.1	103	-	77.0	52.0
CAE 2738	-0.60	30.6	-19.0	41.0	0.60	58.8	34.7
CAE 2770	-0.22	54.4	-12.1	139	0.55	113	62.3

It can be seen for instance from Figure 5.3, where results of test CAD 2750 are presented, that it was rather difficult to determine the second yield point uniquely. It could be that the final unloading was started too early compared to the yield point. Difficulties in determining the second yield points were true for some of the other tests, too. Yield points of first loading were rather evident, instead.

5.1.4 Initial yield curve

Initial yield curve can be fitted to match the observed yield points. In addition to yield points, values of parameters M, α and p'_m are needed in order to fully define the yield surface.

In the case of POKO clay, Näätänen and Lojander (2000) suggested based on triaxial test data that the slope of the critical state line, parameter M, is M=1.1. By the procedure outlined in Section 2.3.1, based on Jaky's simplified formula K_0=0.535 and hence η_{K0}=0.67 and α_{K0}=0.42. Mayne and Kulhawy's (1982) formula would suggest that the in situ K_0=0.605. Most likely, the initial inclination of the yield curve has been created by normally consolidated K_0 loading and the subsequent unloading has been elastic, and hence not rotated the yield curve any further. Therefore, in further

calculations the value of α is based on K_0 from Jaky's simplified formula and not the one corresponding to the current in situ stress state.

The size of the yield curve of POKO clay is p'_m=50 kPa. This value has been determined by fitting the yield curve to the data in Table 5.2 in Section 5.1.3. The yield curve is presented in Figure 5.11.

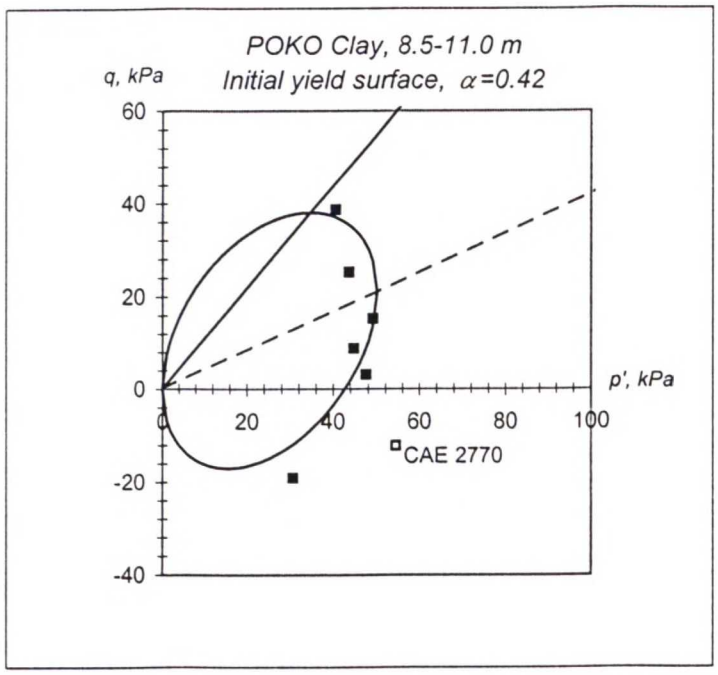

Figure 5.11. *Initial yield surface of POKO clay.*

It is obvious that in Figure 5.11 there is some uncertainty regarding the yield points on extension side. In addition, in the test CAD 2770 where stress ratio was η=-0.22, it was noted that there were air bubbles in the burette while testing was in progress, therefore this point, marked with a different symbol in Figure 5.11, may not be very accurate.

5.1.5 Rotated yield curves

When a sample is loaded to a stress state that lies outside the yield surface, the yield surface starts to enlarge and the inclination of the yield surface tends towards its target value. This target value depends on the current stress ratio.

Therefore, it is possible to plot rotated yield curves for each test on the basis of the value of M, the maximum point at first loading and the second yield point. In this case the size of the yield curve as well as α can be explicitly calculated. The rotated curves are proposed in Figure 5.12. In each figure, the initial yield curve is also presented.

In Figure 5.12, test CAD 2750 has not been included as this was the test where the second loading stage was too short, and therefore it was impossible to determine the yield point. In addition, the η values for the first and second loading were perhaps too close to each other, so any small error in the yield point would suggest a very big error in the determined value of α. In the other tests the rotation of the yield curve seems to go the right direction.

The expected value of α in test CAE 2738 would be negative, but fitting would indicate a positive value of α. Also strange in that particular test is that there is no hysteresis in unloading and reloading that is typical for clays. Therefore, results of this test may not be reliable. Another problem in the test results of Figure 5.12 was that, as mentioned in Section 5.1.4, part of the volume change in test CAE 2770 was air instead of water.

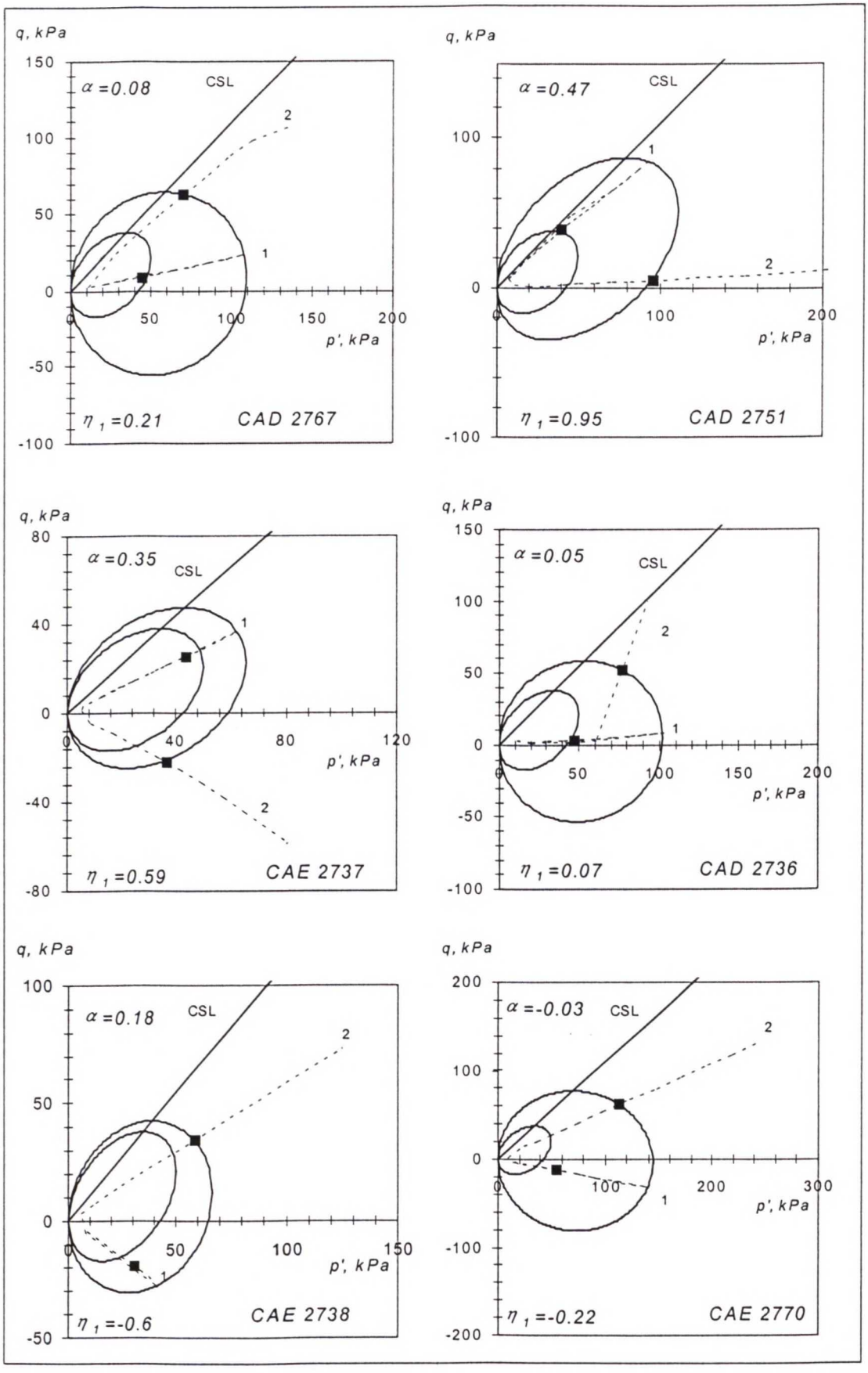

Figure 5.12. *Rotated yield curves of natural POKO clay.*

With the help of the values of α presented in Figure 5.12 the triangular data points in Figure 5.13 are obtained, and the theoretical solution of Equation (2.30) to any combination of η, M and α is also presented. Curves are calculated with four different values of β. Included are also the data points of Otaniemi clay that were originally determined by Näätänen et al. (1999). It can be seen that the data from POKO clay follows the same trend than Otaniemi clay. The points on the extension side make an exception due to the reasons explained in the connection of Figure 5.12.

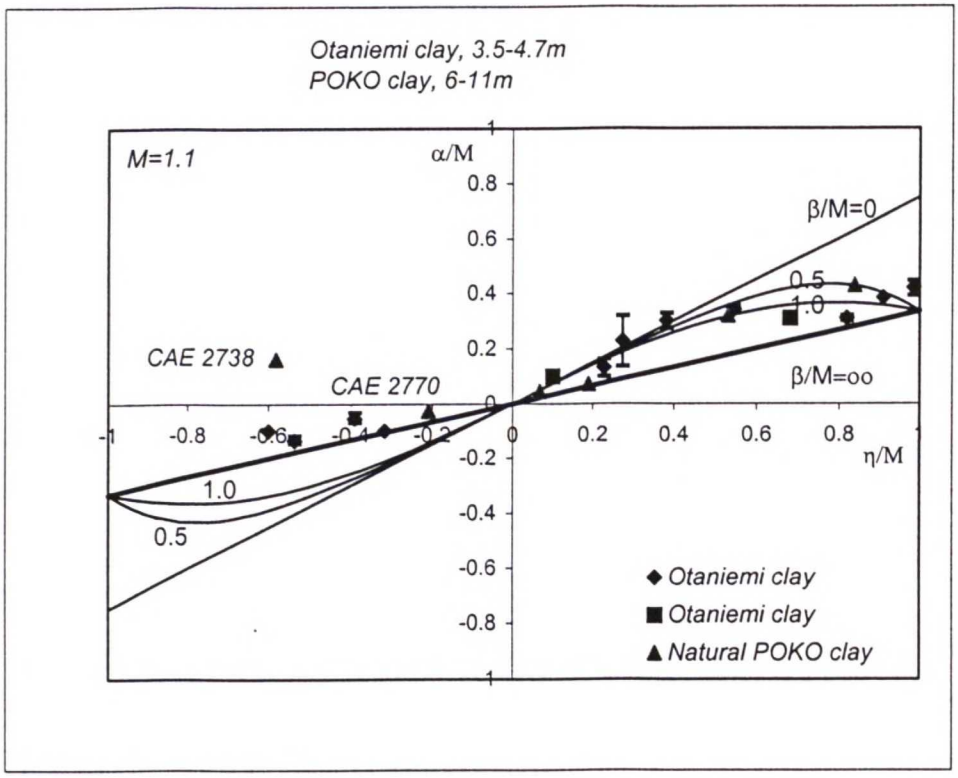

Figure 5.13. *Equilibrium values of α/M.*

5.2 Simulations of tests on natural samples with S-CLAY1

Three triaxial tests were chosen for simulations with S-CLAY1 from the test series on natural samples. They were chosen on the basis of the stress ratios so that one test is nearly isotropic, one test is close to the critical state on compression side and one test is on extension side.

Simulations were done on Microsoft Excel. The anisotropic model S-CLAY1 presented in Chapter 2 was implemented by the author to Excel to calculate the incremental deformations from small loading increments added to the initial state. After each step, the chart updated the stress and deformation state and that state was then used as initial state for calculating the following deformation increment.

In Section 2.3.3 is described a procedure for determining the value of parameter β. For POKO clay, values of M=1.1 and η_{K0}=0.67 give an estimate of β=0.67. Hence, the soil parameters used in the simulations were for all three tests λ=0.86, κ=0.019, M=1.1, α_0=0.42, p'_{m0}=50 kPa, μ=20, β=0.67 and ν=0.2. The value of λ was taken from the oedometer test on natural sample. The initial void ratio and initial stresses were varied from test to test.

Stress increments were chosen to be as small as possible. Increments that were very small increased excessively the amount of rows needed in the chart, and therefore the size of the file. Increments that were too large caused inaccuracies in the calculations. Appropriate size for the mean effective stress increment was found to be about dp'=0.5 kPa and the deviator stress increment was obtained based on the mean effective stress increment and on the stress ratio in each test. The simulated tests are presented in Table 5.3 and the corresponding stress-strain curves in Figures from 5.14 to 5.16 together with the experimental results.

Table 5.3. *Simulated tests on natural POKO clay.*

Test number	p_0' *kPa*	q_0 *kPa*	e_0	*First loading*			*Second loading*		
				η_1	*dp' kPa*	*dq kPa*	η_2	*dp' kPa*	*dq kPa*
CAD 2736	20.3	1.0	2.544	0.07	0.5	0.04	-	-	-
CAE 2738	8.4	-4.9	2.303	-0.6	0.5	-0.34	0.6	1	0.59
CAD 2751	7.2	6.5	2.301	0.95	0.5	0.45	0.055	0.5	0.03

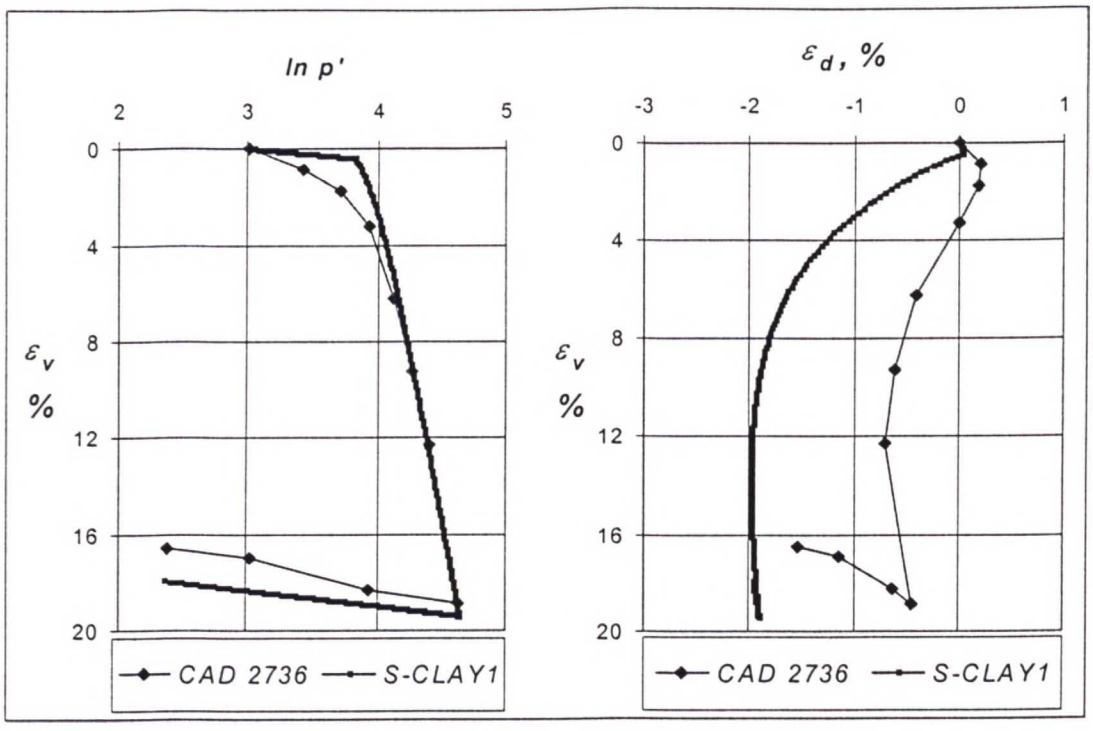

Figure 5.14. *Simulation of test CAD 2736 on natural POKO clay with S-CLAY1, η=0.07.*

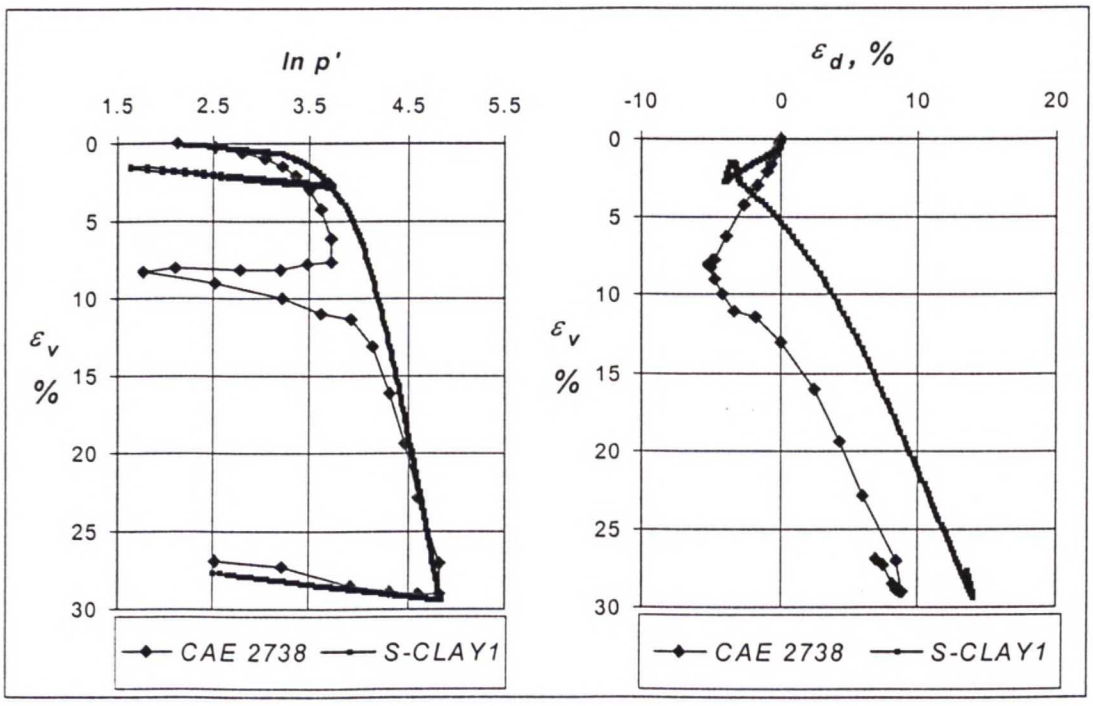

Figure 5.15. *Simulation of test CAE 2738 on natural POKO clay with S-CLAY1, η_1=-0.6 and η_2=0.6.*

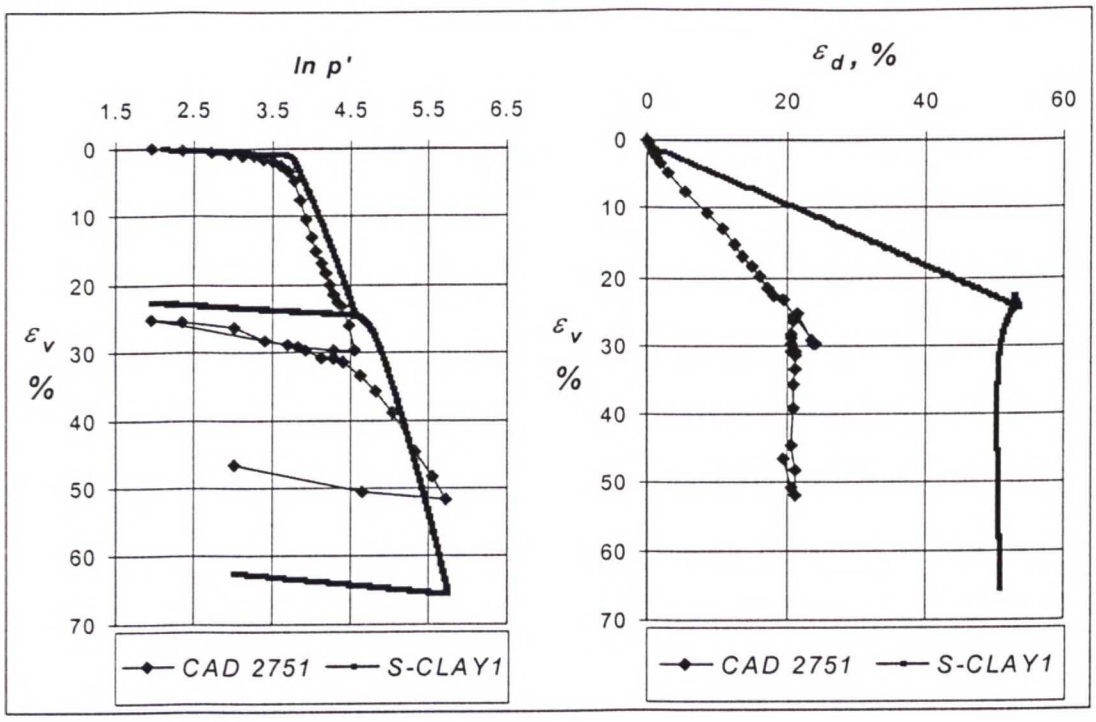

Figure 5.16. *Simulation of test CAD 2751 on natural POKO clay with S-CLAY1, η_1=0.95 and η_2=0.055.*

Simulations of the tests close to critical state (Figure 5.16) and isotropic state (Figure 5.14) seem to be reasonably successful in terms of post-yield volumetric strains during first loading although in the latter case they are slightly underestimated. The simulation of the test on extension side (Figure 5.15) on the other hand highly underestimates the volumetric strain. When volumetric strains are fairly well matched, the shear strains are considerably over-predicted, and when shear strains succeed to be rather close to observed ones, the volumetric strains lie far from the experimental curve. This would suggest that the associated flow rule used in S-CLAY1 is not overall applicable.

On the elastic part of first loading in isotropic test CAD 2736 (Figure 5.14) S-CLAY1 predicts shear strains that tend to the opposite direction than observed positive shear strains. Elasticity seems to be therefore anisotropic as well as plasticity. The yield point, however, is quite well predicted. In unloading stage it is prominent that the observed shear strains are very much larger than predicted ones even though shear strains in this test are quite small. This would indicate again notable elastic anisotropy.

In extension test CAE 2738 (Figure 5.15) the final cumulative volumetric strain in the end of the test is successfully predicted, while the prediction of the first loading fails.

Shear strains of first loading are quite well predicted, but the gradient of strains is not well matched because of failure in prediction of volumetric strains. However, the gradient in second loading is good but shear strains are again slightly overestimated. The shear strains in the elastic region during second unloading are predicted to be going to the opposite direction compared to the observed behaviour, which again would suggest anisotropic elasticity.

The slope and the magnitude of deviatoric strains in the simulation of test CAD 2751 (Figure 5.16) are very poor. Shear strains in this test are quite large due to the big stress ratio, but the model predictions are unrealistically large. Although the volumetric strain in first loading and both yield points are well predicted, during the second loading the volumetric strain is severely over-predicted.

5.3 Test results of reconstituted samples

5.3.1 Test results

The test series of disturbed samples that was introduced in Chapter 4 included four triaxial tests and one oedometer test on reconstituted material. Test results are presented in Figures from 5.17 to 5.20. All the triaxial tests include three loading stages, first of which is K_0 consolidation. The K_0 consolidation is marked in the figures with a solid circle. Second loading is marked with a diamond and the third loading with a triangle. Open marker stands for the corresponding unloading.

The effect of loading time can be seen in the plots as noise. Because of weekends, every fifth loading step took three days instead of one, and therefore, it was sometimes necessary to estimate the one-day values in order to evaluate the parameters correctly. However, the parameter determination was always verified by also determining the parameters with the real measured values.

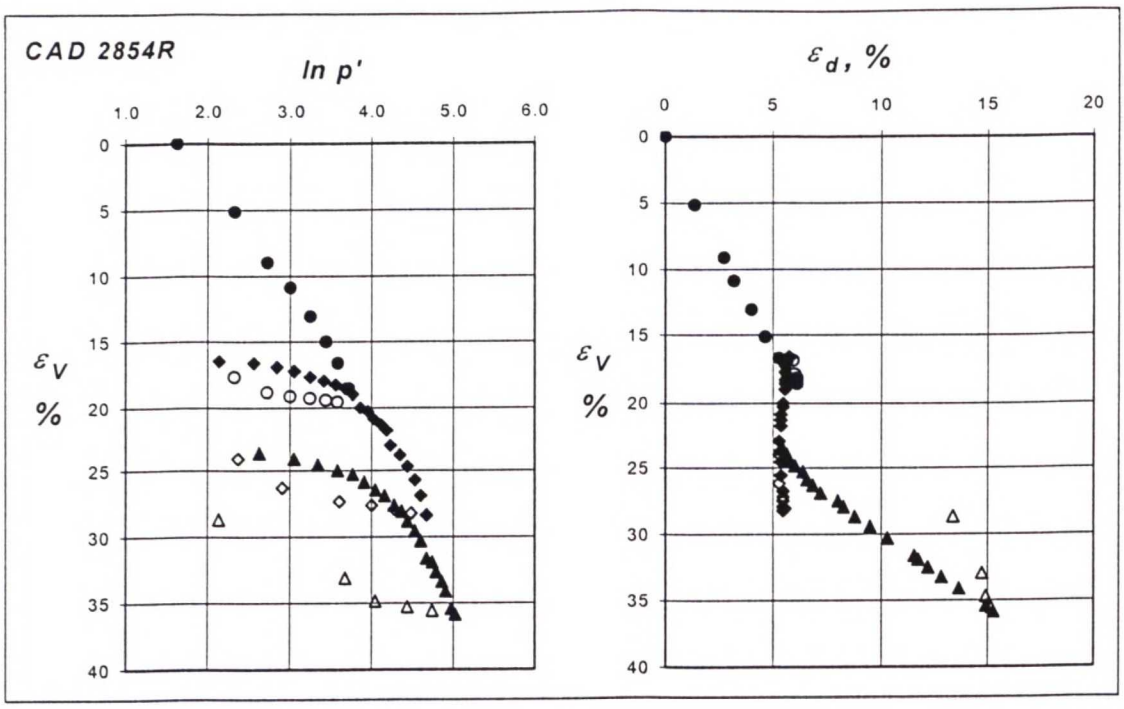

Figure 5.17. *Test CAD 2854R on reconstituted POKO clay, η_1=0.65, η_2=0.21 and η_3=0.88.*

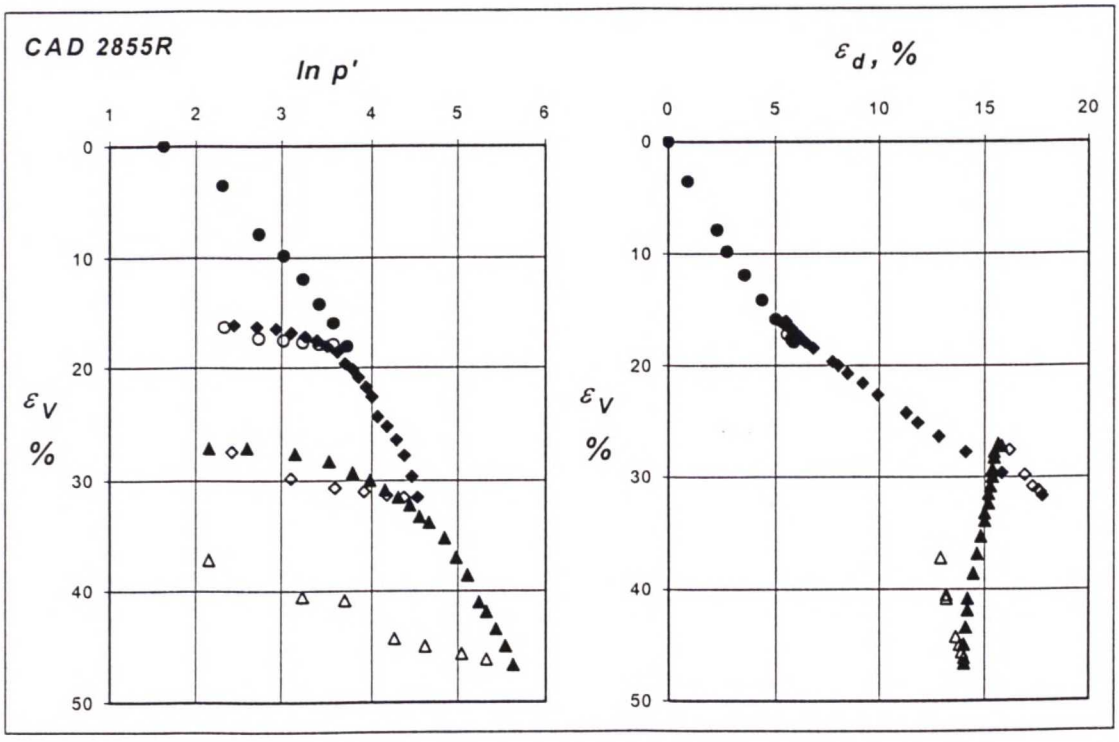

Figure 5.18. *Test CAD 2855R on reconstituted POKO clay, η_1=0.65, η_2=0.91 and η_3=0.05.*

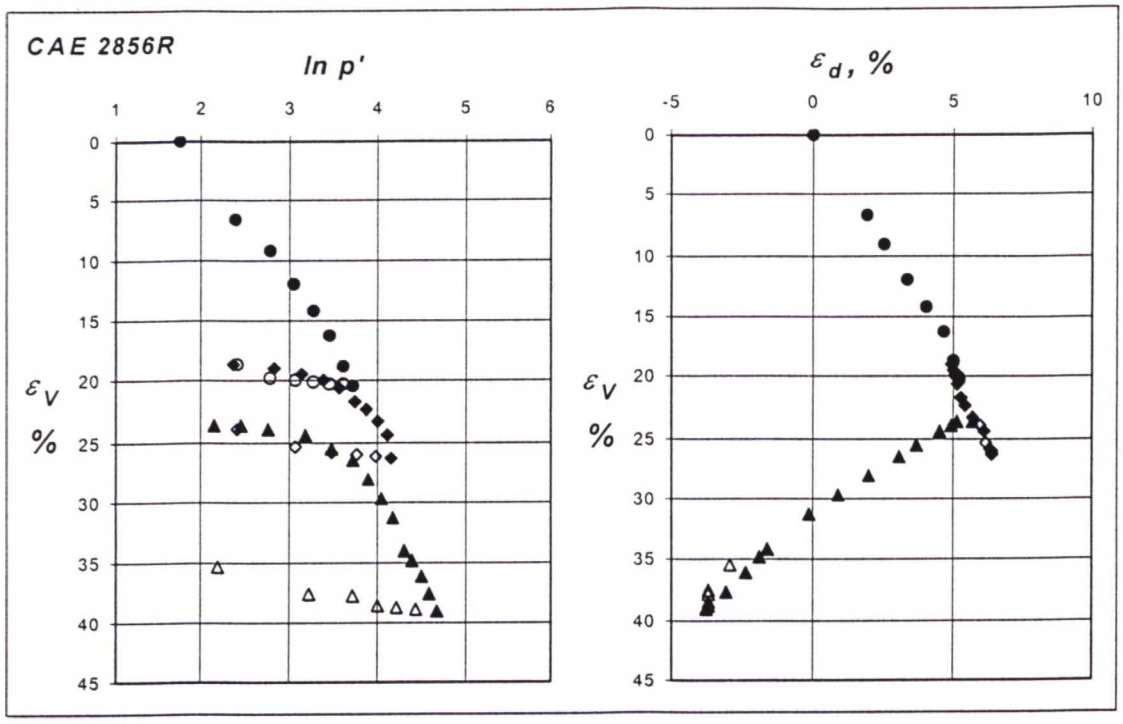

Figure 5.19. *Test CAE 2856R on reconstituted POKO clay, η_1=0.65, η_2=0.59 and η_3=-0.6.*

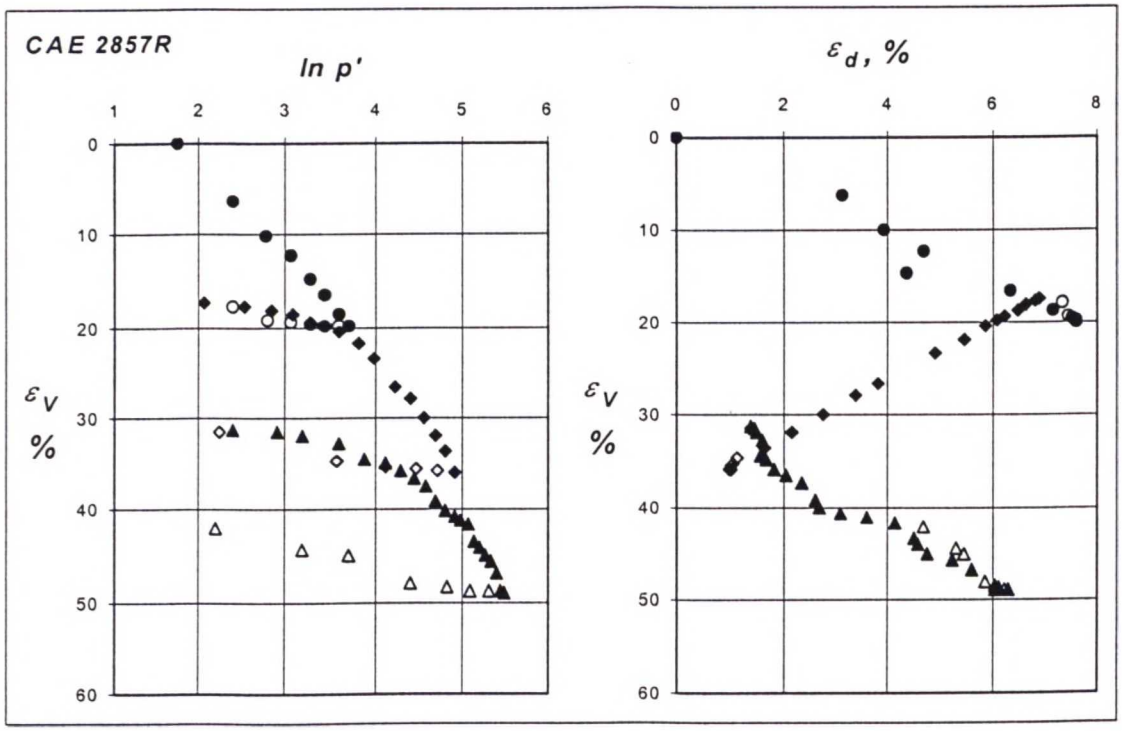

Figure 5.20. *Test CAE 2857R on reconstituted POKO clay, η_1=0.65, η_2=-0.22 and η_3=0.55.*

The oedometer test 2844uR on a reconstituted sample in Figure 5.21 included one loading and unloading. From the second loading step on, the axial strain increased a lot and the points on the σ_1:ε_1 plot form a straight line instead of a curve, which is typical for undisturbed samples.

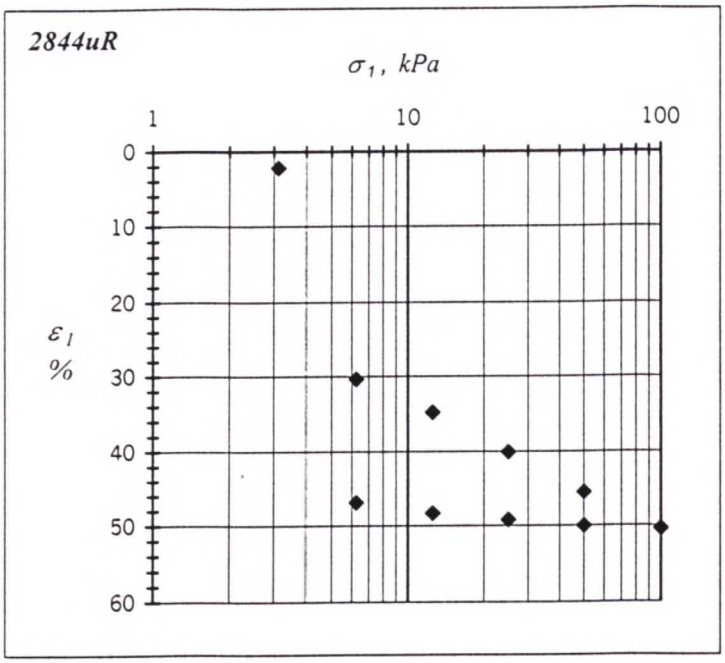

Figure 5.21. *Oedometer test 2844uR on reconstituted POKO clay.*

5.3.2 Parameters λ and κ

One of the main purposes of this work was to determine the intrinsic value of λ for POKO clay. It was determined with the same principles as the values for natural clay, which means determining the slope of the normal consolidation line.

The values of λ for reconstituted clay should be considerably smaller than the values for natural clay, especially in tests with the stress ratio close to critical state. The values of κ should not however vary much. These assumptions are proven to be valid as can be seen from Table 5.4, where the values determined from the tests on reconstituted samples are presented. It can be seen that the intrinsic value of λ is very small compared to the values presented in Section 5.1.2 while the values of κ are about the same

magnitude. The stress paths of first loading were identical in each test in order to imitate the initial K_0 consolidation.

In order to confirm the values of λ and κ, one oedometer test on a reconstituted sample was carried out. Those results are also presented in Table 5.4, and they seem to correspond the other values. This suggests the assumption that these parameters can be determined from oedometer tests for practical design purposes may be acceptable.

Table 5.4. *Values of λ and κ for reconstituted POKO clay.*

Test number	λ	κ
CAD 2854R	0.25	0.019
CAD 2855R	0.27	0.016
CAE 2856R	0.26	0.012
CAE 2857R	0.25	0.015
2844uR (oedometer)	0.30	0.035

It should be noticed that the slopes of normal consolidation lines in each loading stage are rather similar even though the values of λ above were determined merely from the first loading.

5.3.3 Yield points and rotation of yield curve

According to Figures from 5.17 to 5.20, in the first loading no yield point can be found. This is the case due to the reconstitution process and dead weight loading with only 15 kPa axial stress. Even though quite delicate triaxial apparatus was used, this small a yield point was impossible to find. However, yield points could be determined from the second and third loading normally as intersection of unloading-reloading line and normal consolidation line. The determined yield points are presented in Table 5.5.

Table 5.5. *Yield points from tests on reconstituted POKO clay.*

Test number	η_2	p'_{y2}	q_{y2}	η_3	p'_{y3}	q_{y3}
CAD 2854R	0.21	40.9	8.6	0.88	63.8	56.3
CAD 2855R	0.91	33.8	30.9	0.05	90.0	4.7
CAE 2856R	0.59	41.9	24.3	-0.60	40.0	-23.6
CAE 2857R	-0.22	39.1	-8.8	0.55	96.0	53.3

With the help of the yield points presented in Table 5.5 the yield curve representing the initial K_0 consolidation of the reconstituted samples can be plotted. This is possible because the samples were first loaded to the same stress state along the K_0 stress path, and therefore all samples had identical history. The yield curve after first loading is presented in Figure 5.22. The size of the yield curve is best fitted with p'_m=43 kPa.

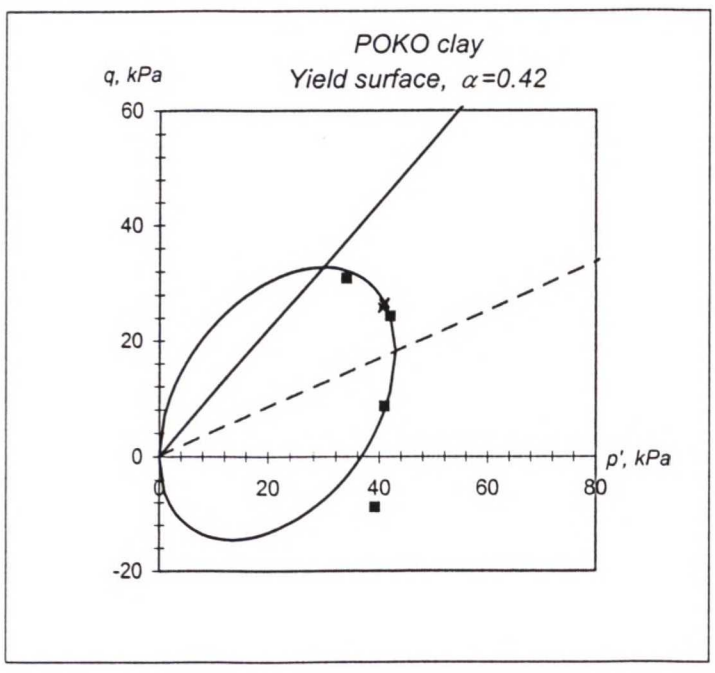

Figure 5.22. *Yield surface of POKO clay after reconstitution and K_0 consolidation.*

Again the point on extension side does not seem to fit the yield curve well. It can partly be attributed to the difficulty of determining the yield point when the yield curve is rotating a lot.

Rotated yield curves can be plotted for each test following the same procedure as for natural samples. The rotation of the yield curve would be expected to be similar as with the natural, structured soil. The rotated curves are presented in Figure 5.23 and as can be seen, the fitted values of α seem reasonably sensible for most of the tests and rotation is evident. Slightly peculiar is test CAD 2854R, which would suggest almost zero value for α. Fitting the yield curve perfectly to the yield point would actually require a negative α value. In this test the stress paths in loading and reloading are both at compression side and fairly close to each other. Any small errors in determining the yield point would significantly affect the value of α.

Further confirmation can be obtained from Figure 5.24, where equilibrium values of α/M for reconstituted samples are presented with open triangles in addition to the data from Figure 5.13. The data points from tests on reconstituted clay fit to the calculated value $\beta/M=0.61$ as well as the rest of the data of POKO and Otaniemi clays and suggest the same trend.

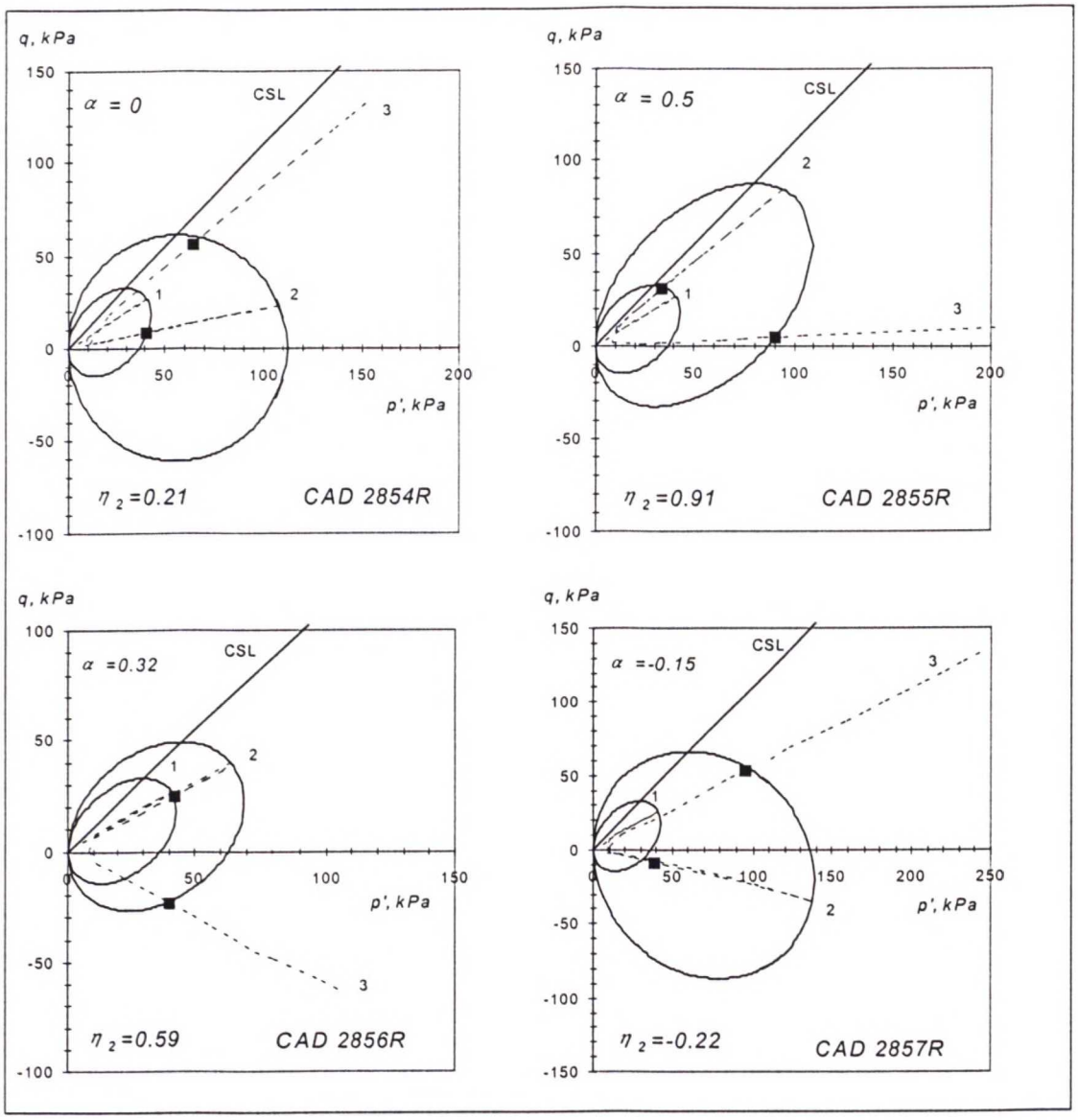

Figure 5.23. *Rotated yield curves of reconstituted POKO clay.*

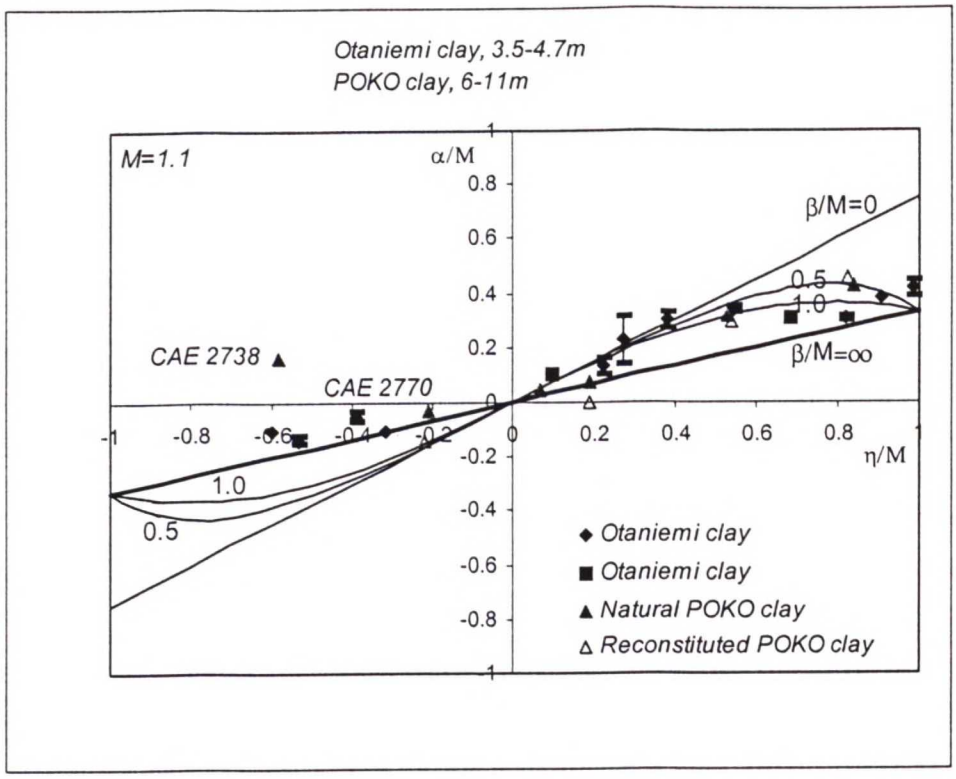

Figure 5.24. *Equilibrium values of a/M.*

5.4 Simulations of the tests on reconstituted samples with S-CLAY1

All the tests in the test series on reconstituted samples were simulated with the anisotropic model similarly to the tests on natural samples previously. In this case the simulation was started from the beginning of the second loading stage. The increment of mean effective stress was held constant as dp'=0.5 kPa and the increment of deviator stress was then calculated based on the stress ratio.

Soil parameters were partly the same as in case of natural test simulations. The two differing parameters were λ, the slope of the normal consolidation line, and p'_{m0}, the initial size of the yield curve. The value of λ used in the simulation was changed into its intrinsic value λ=0.26 and the size of the yield curve according to Figure 5.22, changed to p'_{m0}=43 kPa. Hence, the rest of the parameters are κ=0.019, M=1.1, α_0=0.42, μ=20, β=0.67 and ν=0.2.

The results of the simulations are presented together with the test results in Figures from 5.25 to 5.28.

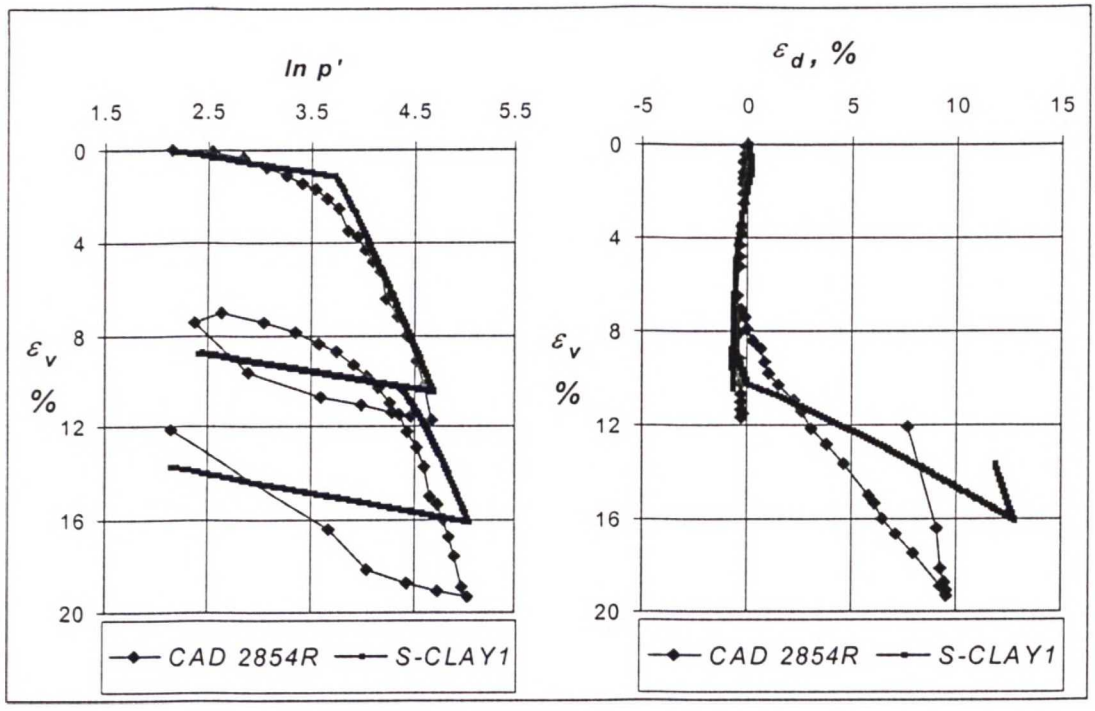

Figure 5.25. *Simulation of test CAD 2854R on reconstituted POKO clay with S-CLAY1, η_2=0.21 and η_3=0.88.*

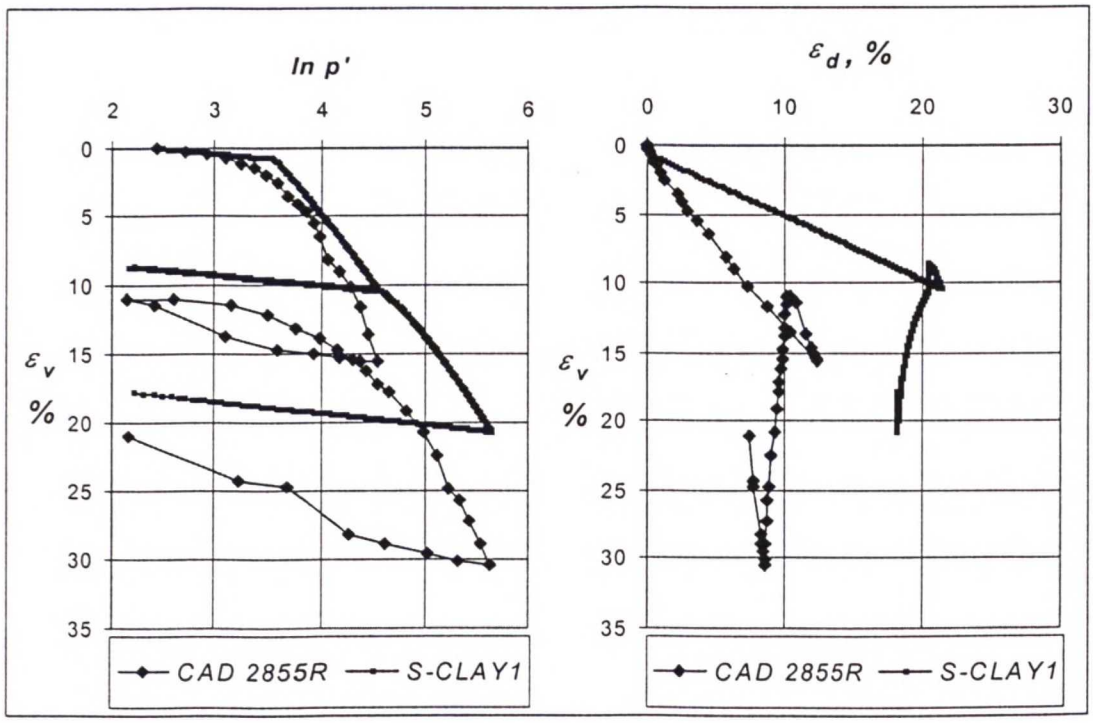

Figure 5.26. *Simulation of test CAD 2855R on reconstituted POKO clay with S-CLAY1, η_2=0.91 and η_3=0.05.*

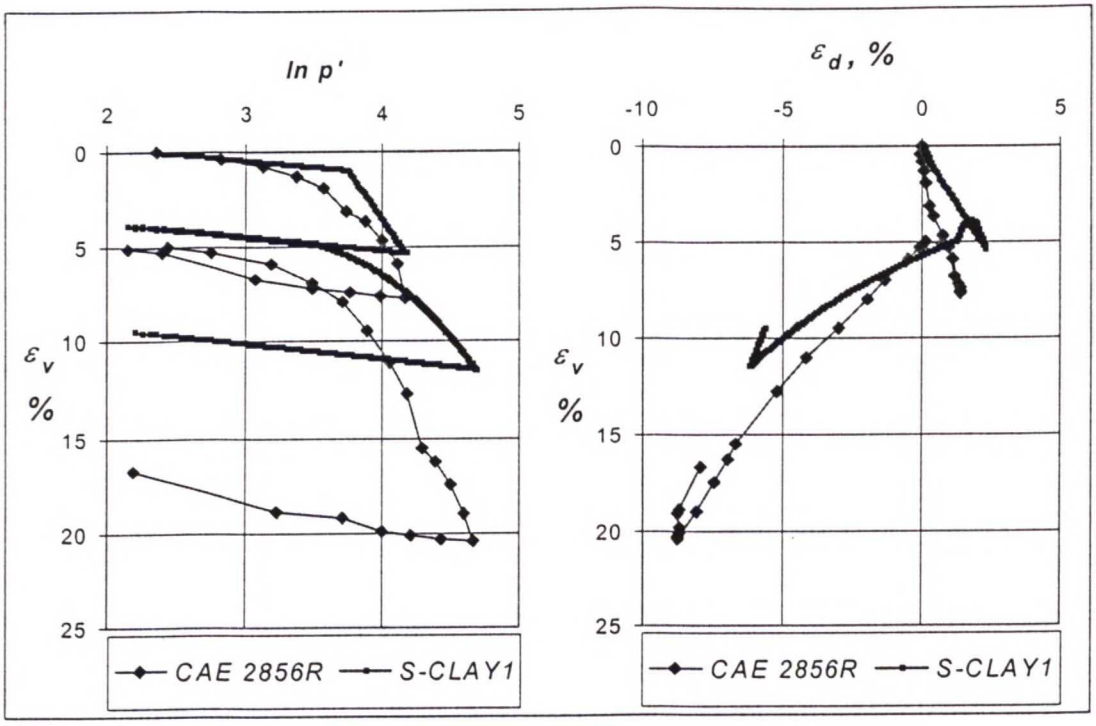

Figure 5.27. *Simulation of test CAE 2856R on reconstituted POKO clay with S-CLAY1, η_2=0.59 and η_2=-0.6.*

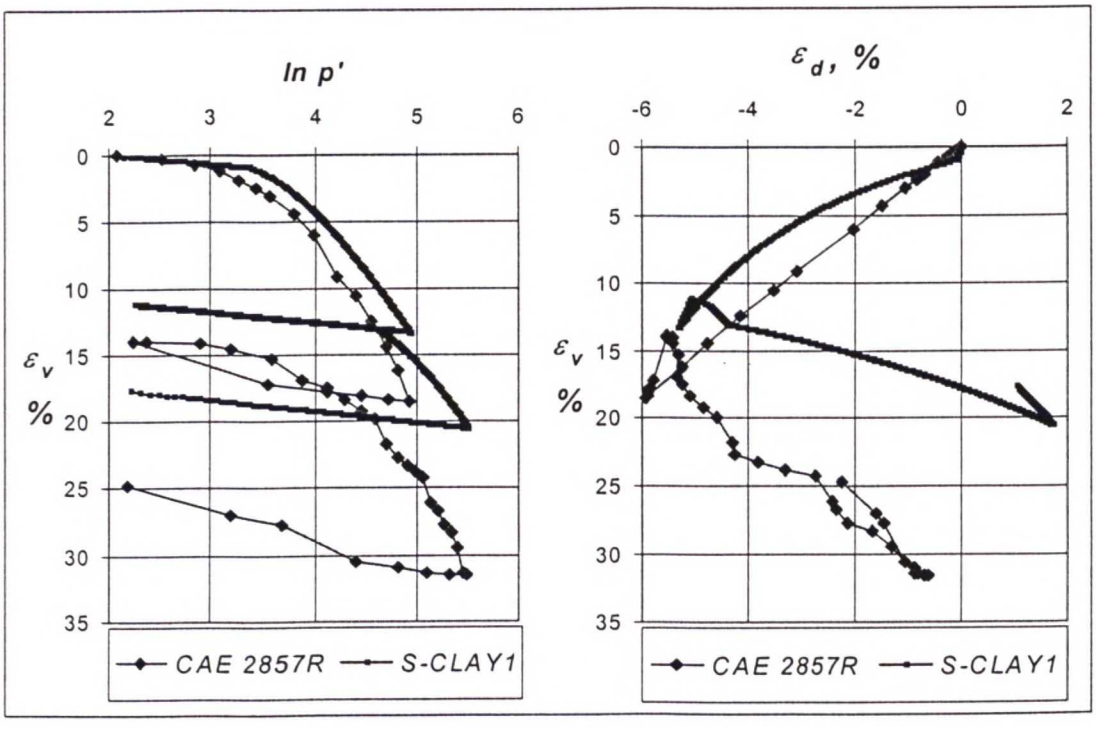

Figure 5.28. *Simulation of test CAE 2857R on reconstituted POKO clay with S-CLAY1, η_2=-0.22 and η_3=0.55.*

The first thing worth pointing out in Figures 5.25...5.28 is that the hysteresis, that is striking in observed unloading and reloading behaviour, is not taken into account by S-CLAY1. This relates to all four simulated tests. In all the tests the first and second yield points are well predicted by S-CLAY1. Differences in other aspects will be next discussed test by test.

Test CAD 2854R in Figure 5.25, which first loading was closest to isotropic state is fairly well simulated when it comes to both volumetric and deviatoric strains and the already mentioned yield points. The gradient of strains in first loading is predicted well, but the gradient of second loading, which is at a high η value, is not as satisfactory and that would suggest that close to critical state the associated flow rule might not be appropriate.

In the rest of the simulations, volumetric strains caused by first loading are not predicted as well as in test CAD 2854R. In this test the loading is closest to isotropic state and hence the model will predict mainly volumetric strains, which according to the model control the changes in the size of the yield curve. This was noticed earlier in the context of simulations of tests on natural samples: anisotropic model S-CLAY1 seems to fit best in terms of volumetric strains for predicting deformations close to isotropic state.

In CAD 2855R (Figure 5.26) volumetric strains are significantly underestimated and shear strains overestimated in first loading. The latter would suggest again that non-associated flow rule should be used instead of associated flow rule. The predicted magnitude of volumetric strain in second loading, again due to the isotropic state, is better, but because of inaccuracy in first loading, the final values do not match well. The underestimation of volumetric strains would suggest that the size of the yield curve depends not only on plastic volumetric strains, but should also be a function of plastic shear strains.

Prediction of volumetric straining in first loading of test CAE 2856R (Figure 5.27) is relatively good even though they are slightly underestimated as in all the simulated tests. Volumetric strains are very much underestimated in second loading, which is in extension. Again shear strains are reasonably well predicted in both loading stages and the gradients of strains are fairly good. This is also a phenomenon that has been seen in previous simulations.

Simulation of CAE 2857R (Figure 5.28) gives a rather good evaluation of first loading especially in terms of the gradient of strains. Even though the slope is quite correct, there is some curvature predicted by the model, which is not visible in the observed results. The slope of second loading is again quite unsuccessful.

In terms of volumetric strains, not very radical improvement can be observed compared to the simulations on tests on natural samples, but slight improvement can be seen between the simulated and observed shear strains. The results suggest that the hardening law related to the size of the yield curve should perhaps depend also on plastic shear strains.

5.5 Simulations of the tests on natural samples with SS-CLAY1

The same three triaxial tests on natural samples were simulated both with S-CLAY1 and with the model that combines the de-structuration with anisotropy in S-CLAY1. The effect of structure was implemented in Microsoft Excel chart with S-CLAY1 as presented in Chapter 3. The principle of calculations followed the incremental elasto-plastic procedure explained in Section 5.2.

Determination of parameters was explained in Chapter 3. The extent of bonding x_0 is initially chosen on the basis of the sensitivity of POKO clay, which varies between 10 and 20, so $x_0=15$ is considered here suitable. Hence, the parameters that were same for all the simulations are $\lambda=0.26$, $\kappa=0.019$, $M=1.1$, $\alpha_0=0.42$, $p'_{m0}=50$ kPa, $x_0=15$, $\mu=20$, $\beta=0.67$ and $\nu=0.2$. Because of taking de-structuration into account, the value of λ is now the intrinsic value determined from the tests on reconstituted samples.

Parameters a and b that cannot be determined directly, were chosen on the basis of simulations. The chosen values of a for testing were 0.5, 1 and 2, and values of b were 1, 2 and 5 based on the work by McGovern (2000) on Otaniemi clay.

Figures from 5.29 to 5.31 present the simulated curves for the case that parameter b equals 5 and different values for parameter a have been assumed.

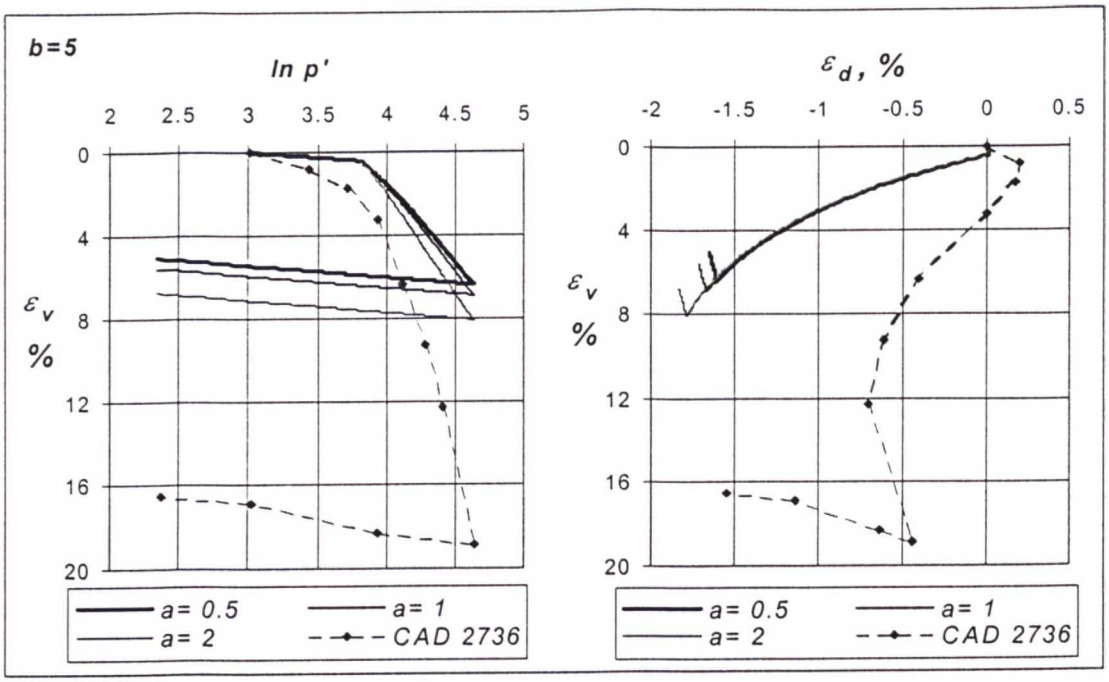

Figure 5.29. *Simulation of test CAD 2736 on natural POKO clay with SS-CLAY1, η_1=0.07.*

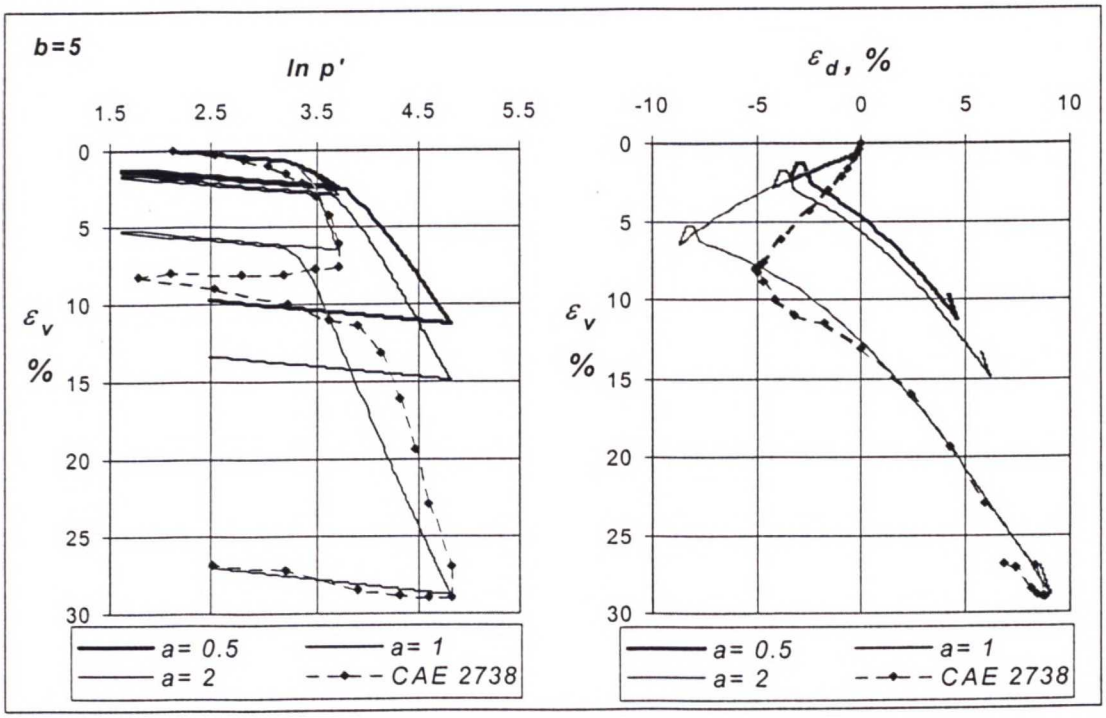

Figure 5.30. *Simulation of test CAE 2738 on natural POKO clay with SS-CLAY1, η_1=-0.60 and η_2=0.60.*

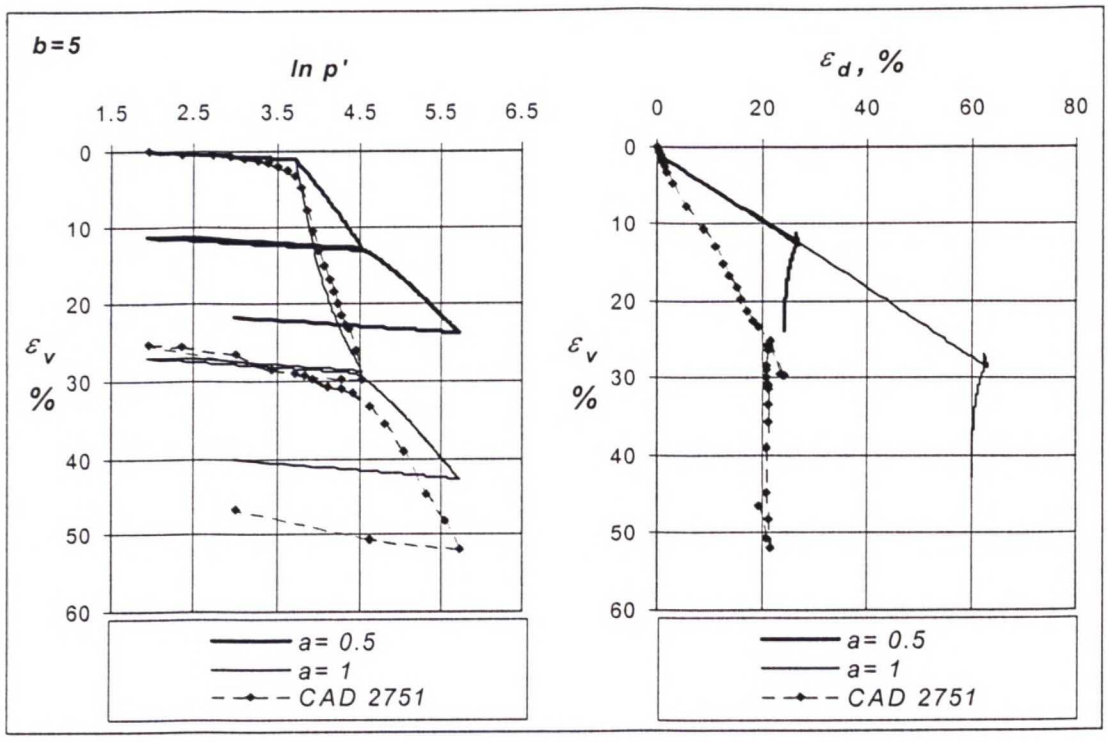

Figure 5.31. *Simulation of test CAD 2751 on natural POKO clay with SS-CLAY1, η_1=0.95 and η_2=0.055.*

The tendency seems to be that the bigger the value of a is, within certain limits, the better is the convergence between the simulated and observed results. The accuracy of the simulation of the second loading has also improved slightly in some cases.

Simulation of isotropic test CAD 2736 with SS-CLAY1 (Figure 5.29) is not as good as the simulation with anisotropic model S-CLAY1. This test has an isotropic stress path that will introduce only minor degrading of structure in the soil. Changing parameter a in the chosen limits does not help in improving the prediction, so radical changes in x_0 and b would be required.

In extension test CAE 2738 (Figure 5.30) the effect of parameter a is more significant. Smaller values of parameter a clearly underestimate volumetric strains and, in some degree, shear strains as well. Selecting a=2 gives a good prediction of volumetric strain, but slightly overestimated result of shear strains. Second yield point is predicted inaccurately and as for first loading, the gradients of strains do not match either. In second loading the total volumetric and shear strains and the gradient of strains are well

predicted. What is also notable is the opposite elastic behaviour of the prediction compared to the experimental observation in second unloading.

Test CAD 2751 (Figure 5.31) was loaded along a rather steep stress path. Therefore, the de-structuration effect is more significant than in other simulated tests and hence SS-CLAY1 is capable of predicting well the behaviour of volumetric strains in this test. Combination of a=2 and b=5 gave an irrational prediction, and therefore it is not presented in Figure 5.31. Changing parameter a from 0.5 to 1 shows a big difference in predicted curves. Because parameter a is a rate parameter of de-structuring effect in soil, this means that when the magnitude of de-structuration is large, a small increase in the rate, i.e. parameter a, has a big effect on predictions.

Prediction of pattern of straining in CAD 2751 would again argue for a non-associated flow rule. When volumetric strains are predicted well, shear strain predictions fail and vice versa.

The next step was to select the best value of a in each test on the basis of previous simulations, and study the effect of changing parameter b. Value a=2 was chosen. The results for b values of 1, 2 and 5 are presented in Figures from 5.32 to 5.34.

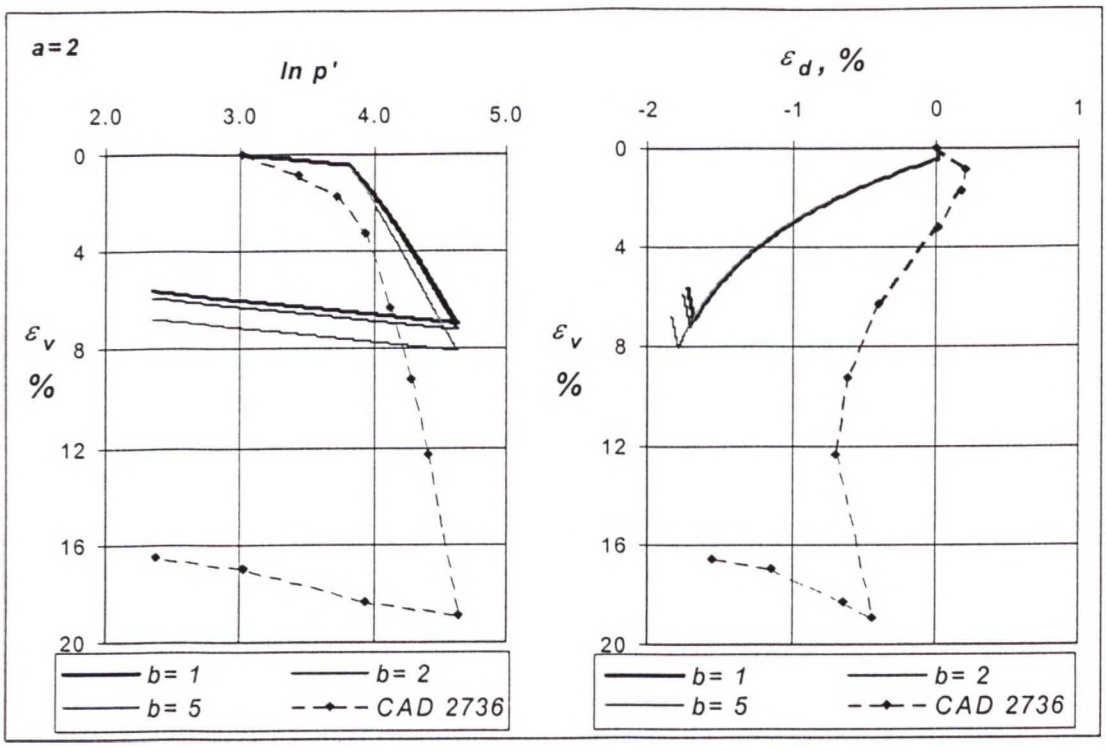

Figure 5.32. *Simulation of test CAD 2736 on natural POKO clay with SS-CLAY1, η_1=0.07.*

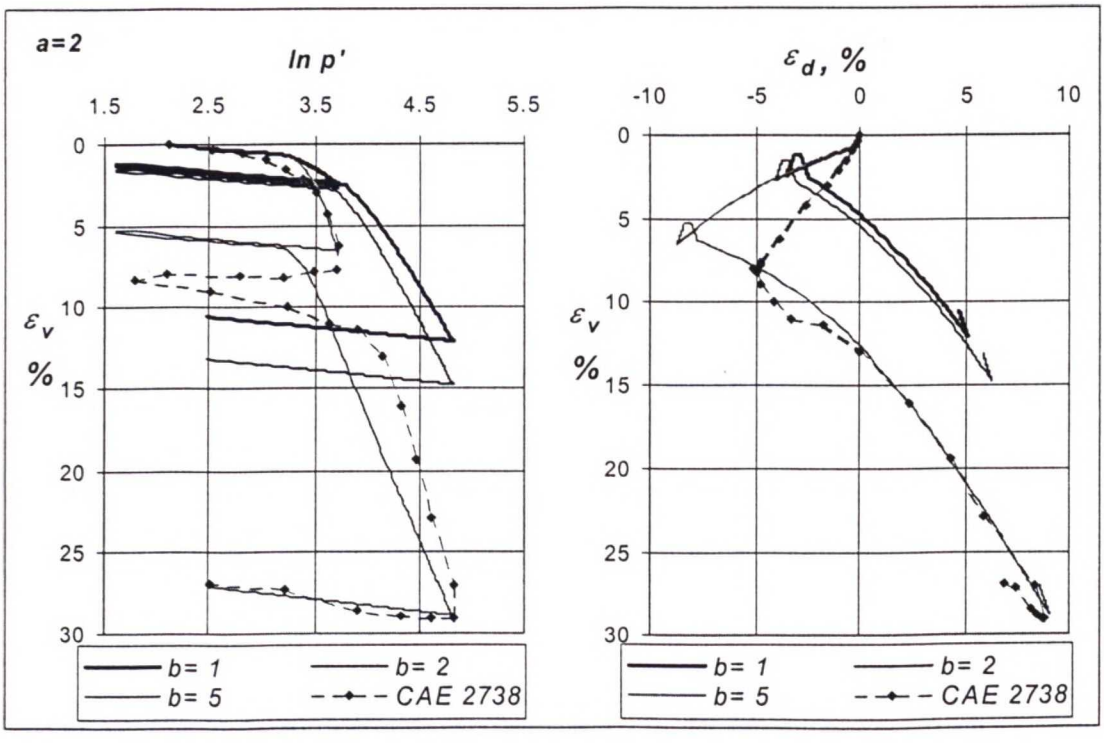

Figure 5.33. *Simulation of test CAE 2738 on natural POKO clay with SS-CLAY1, η_1=-0.60 and η_2=0.60.*

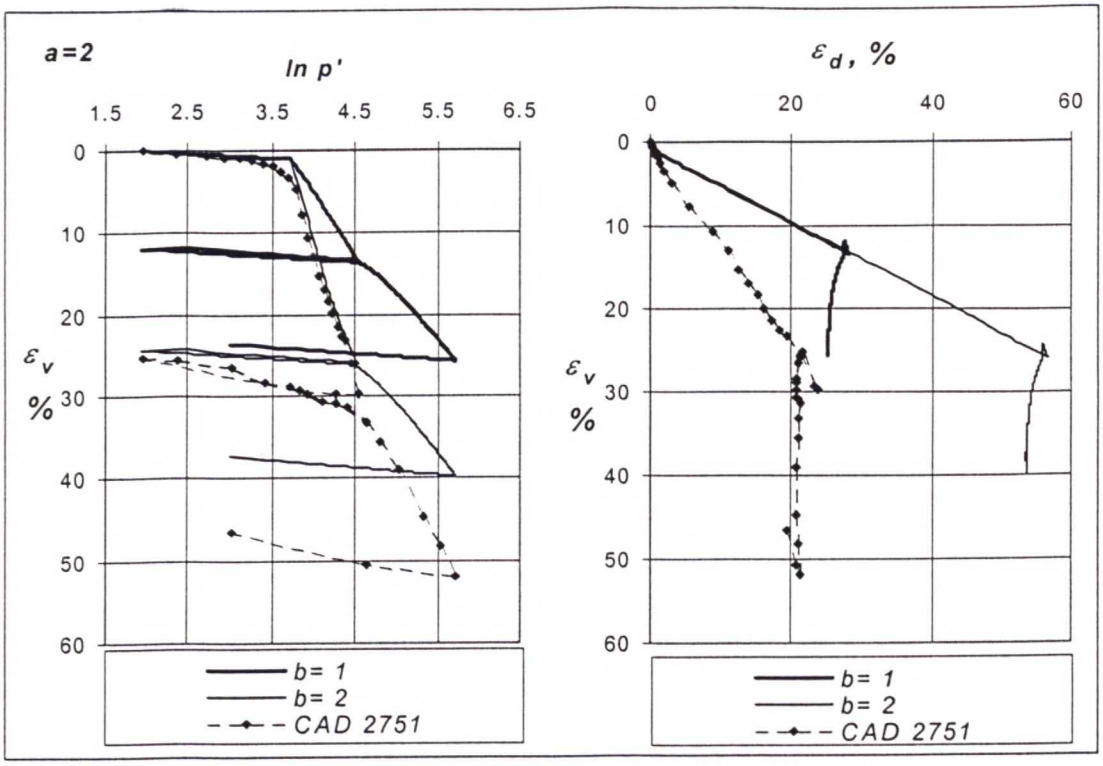

Figure 5.34. *Simulation of test CAD 2751 on natural POKO clay with SS-CLAY1, η_1=0.95 and η_2=0.005.*

In Figure 5.34, the simulated curve with b=5 is missing for the same reason as the combination a=2 and b=5 was missing from Figure 5.31.

Parameter b controls the effectiveness of shear strains in relation to volumetric strains in degrading the structure in soil. There can be seen no major improvement in using the smaller values of parameter b in simulations. Therefore, according to these results, it can be said that the best combination of parameters a and b is b=2...5 and a=1...2, but this cannot be applied generally to all simulations. At the current development stage of the model, parameters a and b must be considered individually according to the stress path, among other things, which of course is not appropriate for design purposes.

There is still one parameter that may require testing. That is x_0, which was chosen on the basis of the sensitivity of POKO clay. In Figures from 5.35 to 5.37 the effect of changing x_0 with the best combination of parameters in each test is studied.

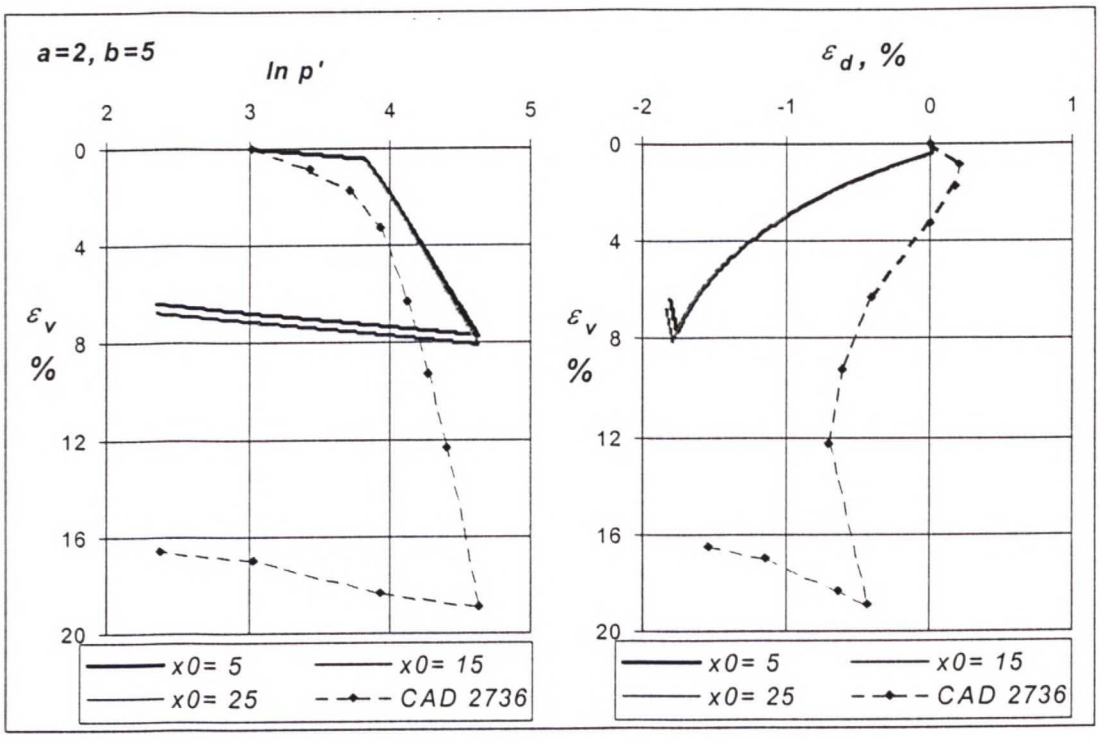

Figure 5.35. *Simulation of test CAD 2736 on natural POKO clay with SS-CLAY1, η_1=0.07.*

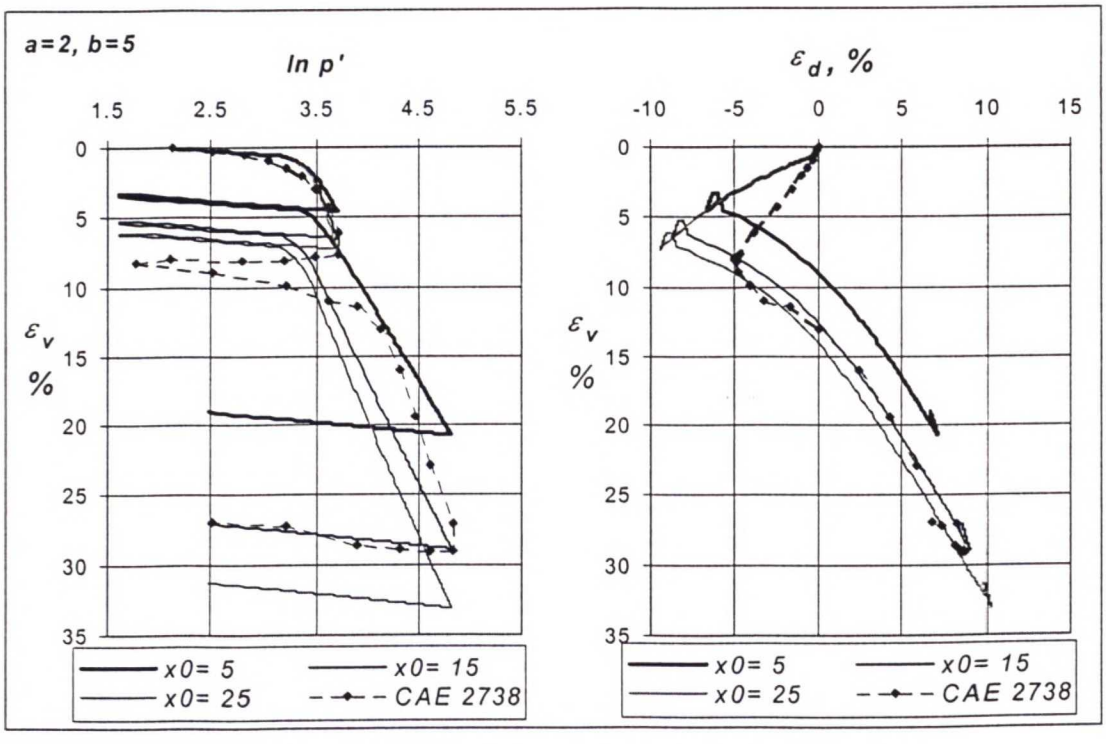

Figure 5.36. *Simulation of test CAE 2738 on natural POKO clay with SS-CLAY1, η_1=-0.60 and η_2=0.60.*

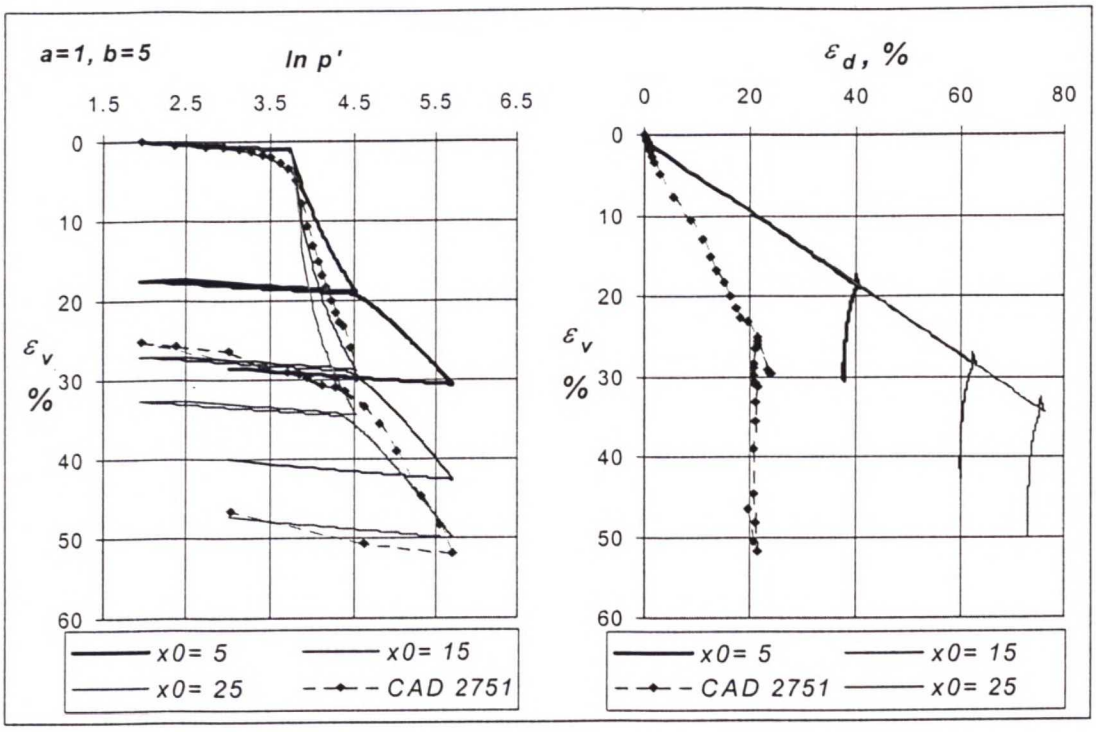

Figure 5.37. *Simulation of test CAD 2751 on natural POKO clay with SS-CLAY1, η_1=0.95 and η_2=0.055.*

The effect of changing x_0 is minor in test CAD 2736 (Figure 5.35) assumingly because the test was isotropic and hence the effect of de-structuration was not very significant. Instead, the simulations of tests CAE 2738 (Figure 5.36) and CAD 2751 (Figure 5.37) show quite large shift in the curve in terms of predicted volumetric strains when x_0 is changed. These tests are at stress paths that are closer to critical state and therefore de-structuration is more dominant than in CAD 2736. An x_0 value of 15...20 would seem most appropriate.

The shape of the ln p':ε_v curve expresses how vigorous the de-structuration is as well. If there is a sharp corner as is in CAD 2751 (Figure 5.37), the effect of structure is strong, and when the shape of the curve is smooth (Figure 5.36), anisotropy is dominant.

In the isotropic test CAD 2736 simulation would be remarkably better if the value of λ would be bigger than the λ=0.26 that is used.

6. CONCLUSIONS AND RECOMMENDATIONS

The aim of this work was to study the effect of anisotropy and structure on the behaviour of soft clays. This was done by testing both reconstituted and natural samples with triaxial equipment and then simulating these tests both with a constitutive model that features the anisotropy (S-CLAY1) and a model that combines the effects of anisotropy and structure (SS-CLAY1).

The main testing programme with natural POKO clay included seven triaxial consolidation tests and some oedometer tests first on natural undisturbed samples in order to confirm the appropriate values of parameters. The consolidation test programme was planned to give enough information for determining the size and shape of the initial yield surface for POKO clay, and therefore several different constant radial stress paths for first loading were used. Secondly, the rotation of yield surface due to subsequent loading was studied.

A rehearsal test programme with reconstituted samples of Bothkennar clay as well as the main programme on reconstituted samples of POKO clay gave valuable information about the suitable sample preparation procedure for making consistent reconstituted samples from different clays. The best way for reconstituting clay was found to be the one suggested by Burland (1990): remoulding soft soil in a water content that is higher than natural. After reconstituting, one-dimensional consolidation is required in order to solidify the sample enough for testing in the laboratory the same way as natural undisturbed soil. The consolidation time should be determined so that primary consolidation has ended, and this can be confirmed either with logarithm of time or square root of time fitting methods (Atkinson 1995). After primary consolidation the sample is well manageable. If it is extruded too early it can be too soft and suffer from damage during testing preparations.

It could be shown that the value of λ depends on the stress path, and furthermore it very strongly depends on the structure present in the soil. Loading a natural sample with a high stress ratio causes rapid de-structuring effect in the sample and therefore the slope of the normal consolidation line is steeper than with stress paths that are closer to isotropic state. This effect cannot be noted in the slope of the overconsolidation line, so the phenomenon of de-structuration is mainly attributable to plastic strains.

Reconstitution reverts the sample to its intrinsic properties in which the structure is not present. The effect can be seen especially in the value of λ, but is not noted in the critical state parameter M or the value of κ. The size of the de-structured yield curve is suggested to be derived based on the size of the initial yield curve and the value for sensitivity of the soil.

The simulations with the anisotropic model S-CLAY1 underestimate the volumetric strains and overestimate the shear strains or vice versa depending on the choice of λ and the stress paths considered. S-CLAY1 works for isotropic stress paths and for the reconstituted samples, and therefore it is a reasonable assumption that after implementing de-structuration in it the predictions would improve.

Nevertheless, the combined model SS-CLAY1 shows no significant improvement in ability to predict the strains generally. The weakness of associated flow rule is still visible in SS-CLAY1 for certain stress paths. This leads to a situation where either prediction of volumetric strains or shear strains fail. One solution could be dividing the shear strains in two parts: the ones caused by anisotropy and the ones caused by de-structuration and assume a flow rule (non-associated) that would predict the magnitude of plastic shear strains based on the plastic volumetric strains due to anisotropy.

The use of S-CLAY1 or SS-CLAY1 and the parameters a and b in latter model need to be thought over individually for every situation. This may lead to too large testing programmes and is not practical to use.

Based on the results presented here, a question is raised, if the formulation of the hardening law considering the structural degradation is quite correct as well as if the fundamental assumptions relating to the evolution of the size of the yield curve are correct.

The prediction of second loading stage is quite inaccurate with both models, which might date back to the poor ability, even of the combined model, in predicting the development and erasure of structure under loading.

This project was the first attempt to combine anisotropy and structure in a combined framework supported by systematic experimental test on both natural and reconstituted samples. There are still many questions about both soil models, S-CLAY1 and SS-

CLAY1, discussed in this work. Despite this, the two models represent positive development and improvement to the current state of the art in modelling the behaviour of soft natural soil.

REFERENCES

Atkinson, J.H., 1995. Incremental loading oedometer test on water-saturated soil. XI ECSMFE, Workshop 2: Standardisation of laboratory testing, Copenhagen, 28 May – 1 June, p. 45-62.

Banerjee, P.K., Yousif, N.B., 1986. A plasticity model for the mechanical behaviour of anisotropically consolidated clay. International Journal for Numerical and Analytical Methods in Geomechanics 10, p. 521-541.

Berre, T., 1995. Methods for triaxial compression tests on water-saturated soils. XI ECSMFE, Workshop 2: Standardisation of laboratory testing, Copenhagen, 28 May – 1 June, p. 27-44.

Burland, J.B., 1990. On the compressibility and shear strength of natural clays. Géotechnique 40, No. 3, p. 329-378.

Christoulas, S. (ed.), 1987. Embankments on soft clays. Bulletin of the public works research centre, Athens, 358 p.

Dafalias, Y.F., 1987. Anisotropic critical state clay plasticity model. Proc. of 2nd int. conf. on constitutive laws for engineering materials, Tucson, Arizona, Vol. I, Elsevier, p. 513-521.

Davies, M.C.R., Newson, T.A.A., 1993. Critical state constitutive model for anisotropic soils. Predictive soil mechanics (Eds. G.T. Houlsby and A.D. Schofield), London, Thomas Telford, p. 219-229

Gens, A., Nova, R., 1993. Conceptual bases for a constitutive model for bonded soils and weak rocks. Proc. of int. symp. of hard soils – soft rocks, Athens, 10 p.

Hight, D.W., Bond, A.J., Legge, J.D., 1992. Characterization of the Bothkennar clay: an overview. Géotechnique 42, No. 2, p. 303-347.

Karstunen, M., 2000. Elasto-plastic matrix. SCMEP, Workshop 1, Trondheim, Norway, 27-30 August, 14 p.

Karstunen, M., Näätänen, A., Wheeler, S., 2001. Simulations of soft clay behaviour with S-CLAY1 and MCC. Proc of 10th Int. Conf. of Computer Methods and Advances in Geomechanics, Tucson, Arizona, 7-12 January, 4 p.

Korhonen, K-H., Lojander, M., 1987. Yielding of Perno clay. Proc of 2nd Int. Conf. On Constitutive Laws for Engineering Materials, Tucson, Arizona, Vol. 2, Elsevier, p. 1249-1255.

Leroueil, S., Magnan, J-P., Tavenas, F., 1999. Embankments on soft clays. 360 p.

Leroueil, S., Vaughan, P.R., 1990. The general and congruent effects of structure in natural soils and weak rocks. Géotechnique 40, No. 3, p. 467-488.

Liu, M.D., Carter, J.P., 2000. Modelling the destructuring of soils during virgin compression. Géotechnique 50, No. 4, p. 479-483.

Mayne, P.W., Kulhawy, F.H., 1982. K_0-OCR relationship in soil. Journal of the Geotechnical Engineering Division, Vol. 108, GT6, p. 851-872.

McGinty, K., 2000. Personal communication, University of Glasgow.

McGovern, G.W., 2000. Constitutive modelling of anisotropy and de-structuration in natural soft clays. Master's Thesis, Department of Civil Engineering, University of Glasgow.

Näätänen, A, Lojander, M., 2000. Modelling of anisotropy of Finnish clays. VII Suomen mekaniikkapäivät, Tampere, 25.-26.5., s. 589-598.

Näätänen, A., Lojander, M., Wheeler, S., Karstunen, M., 1999. Experimental investigation of an anisotropic hardening model for soft clays. Proc. of the 2nd International Symposium on Pre-failure Deformation Characteristics of Geomaterials, Torino, Italy, 28-30 September, Rotterdam, A.A. Balkema, p. 541-548.

Paul, M.A., Peacock, J.D., Wood, B.F., 1992. The engineering geology of the Carse clay at the National Soft Clay Research Site, Bothkennar. Géotechnique 42, No. 2, p. 183-198.

Pestana, J.M., Whittle, A.J., 1999. Formulation of a unified constitutive model for clays and sands. International Journal for Numerical and Analytical Methods in Geomechanics 23, p. 1215-1243.

Roscoe, K.H., Burland, J.B., 1968. On the generalized stress-strain behaviour of 'wet' clay. Engineering plasticity, Cambridge University Press, p. 553-609.

Wheeler, S.J., 1997. A rotational hardening elasto-plastic model for clays. Proc. of the XIV ICSMFE, Hamburg, Vol. 1, Rotterdam, A. A. Balkema, p.431-434.

Wheeler, S.J., 2000. Modelling of de-structuration of soft clays. Presentation at SCMEP, Workshop 1, Trondheim, Norway, 27-30 August.

Wheeler, S., Karstunen, M., Näätänen, A., 1999. Anisotropic hardening model for normally consolidated soft clays. Proc. of NUMOG VII, Graz, Austria, 1-3 September, Rotterdam, A.A. Balkema, p. 33-40.

Wheeler, S., Näätänen, A., Karstunen, M., Lojander, M., 2000. An anisotropic elasto-plastic model for natural soft clays. SCMEP, Workshop 1, Trondheim, Norway, 27-30 August, 30 p.

Whittle, A.J., Kavvadas, M.J., 1994. Formulation of MIT-E3 constitutive model for overconsolidated clays. Journal of Geotechnical Engineering 120(1), p. 199-224

Wood, D.M., 1990. Soil Behaviour and Critical State Soil Mechanics. Cambridge University Press, 462 p.